Initial sardine projections based on constant catch scenarios

C.L. de Moor*

Correspondence email: *carryn.demoor@uct.ac.za*

Introduction

In December 2018 the Small Pelagic Scientific Working Group (SWG-PEL) declared Exceptional Circumstances for the sardine resource as a result of (among other things) the very low survey estimate of sardine abundance in November 2018. Any Total Allowable Catch/Bycatches (TAC/Bs) that would have been recommended under OMP-18 were thus set aside. The SWG-PEL recommended a delay in the start of the directed sardine fishery to allow further computations to be undertaken to assess whether some non-zero directed sardine TAC could be scientifically justified for 2019.

This document considers some projections of the sardine resource under alternative constant catch scenarios to initiate discussions towards the possible increase of 2019 sardine TABs and/or the setting of a 2019 directed sardine TAC.

Methods

The model used for projections is based on the most recent updated assessment of the sardine resource (de Moor 2019). Most of the population dynamics are similar to those assumed historically (Appendix A) except that catch is modelled to be taken in a single pulse during the year. Other assumptions made during these projections are listed in Appendix A.

There are three potential main uncertainties in these projections that have been highlighted by the sardine task team (STT), namely future recruitment to the population, future movement of west component fish to the south component and the November 2018 abundance.

Future recruitment

Figure 1 shows the model predicted recruitment against the effective spawning biomass. 8% of south coast spawning biomass is assumed to contribute to the west component effective spawning biomass (de Moor 2019). The south component effective spawning biomass is thus 92% of the south component spawning biomass. The recruitment to the west component has previously been shown to be the major contribution of recruitment to the population as a whole (de Moor *et al.* 2017). Fitting a hockey stick stock recruitment relationship indicates there is no clear dependence of recruitment on effective spawning biomass. This apparent lack of relationship is robust to fitting a relationship over a) all non-pulse years, b) to 2005-2017 only, or c) only to 'data' points corresponding to low (<100 000t) effective west component spawning biomass. Figure 2 shows the same 'data' plotted against time, indicating some potential changes in 'recruitment regimes' over time. Results are initially shown assuming deterministic hockey-stick stock recruitment curves, even though this assumption could be considered to be unrealistic for a small pelagic species. Two alternatives of future recruitment are considered herein:

i) Future recruitment is generated from a hockey-stick stock recruitment curve fitted to all non-pulse curves, with a variability of $\sigma_R = 0.85$ estimated from the fit to the historical west component point estimates.

* MARAM (Marine Resource Assessment and Management Group), Department of Mathematics and Applied Mathematics, University of Cape Town, Rondebosch, 7701, South Africa.

This method ignores the possible trend in residuals (Figure 1). Furthermore, Cox *et al.* (2018) recommended future recruitments be drawn from past residuals, after having accounted for any auto-correlation between residuals.

ii) Future recruitment is generated from the past 5 years of recruitment under the assumption that future recruitment, particularly in the immediate short-term future, may be from a similar regime to that of the more recent 5 years.

The past 5 years has been selected as 5 and 10 years are frequent choices for the "recent past" in similar analyses internationally.

Future movement

A fixed time-invariant proportion of 1-year-olds are assumed to move from the west component to the south component each year. The proportion of 2+ year olds which move is 47% of that of the 1-year old proportion (de Moor 2019). Three alternative proportions of 0.1, 0.3 and 0.5 are considered here. In the past 10 years, the point estimates of movement were estimated to be between 0.0 and 0.88, with an average of 0.24. Additionally, if a density-dependent hypothesis were assumed (de Moor e*t al.* 2018), one would expect movement in the short-term to be relatively low.

November 2018 abundance

The initial assessment model's predicted survey estimates of sardine biomass in November 2018 were above that observed (de Moor 2018). These are point estimates only and no posterior distributions have been calculated. Two alternative starting points were considered herein:

i) The assessment model's numbers-at-age in 2018, which correspond to a predicted survey biomass of 46 000t west of Cape Agulhas and 204 000t south of Cape Agulhas. These are larger than the survey estimates of 35 000t sardine west of Cape Agulhas and 56 000t south of Cape Agulhas.

ii) A decrease in the assessment model's numbers-at-age in 2018 corresponding to 1 standard error based on the survey CVs. The west component numbers-at-age are decreased to 1-0.3591=0.64 of the assessment point estimates and the south component numbers-at-age are decreased to 1-0.7828=0.22 of the assessment point estimates. The corresponding predicted survey biomasses were 29 000t west of Cape Agulhas and 44 000t south of Cape Agulhas.

Projections are made assuming a 5000t small sardine bycatch or a 10 000t small sardine bycatch (results in Appendix C). Variability is introduced by running 100 simulations.

Results and Discussion

Figures 3 to 5 show the model predicted effective west and south component spawning biomass assuming future recruitment is according to a deterministic hockey stick stock recruitment relationship. The deterministic trajectories indicate that the population is able to support all the alternative constant catch/bycatch scenarios tested. This is because the general lack of dependence of recruitment on spawning biomass (Figure 1) results in future west component recruitment being assumed to be ~20 billion recruits in almost all simulations/years. However, small pelagic species are well known for their highly variable recruitment.

The scenarios with lower/higher west to south movement resulted in higher/lower 2019 and equilibrium biomass for the west component and lower/higher biomasses for the south component.

The lower starting point scenario resulted in lower 2019 projected biomass values (after the full constant catch levels are modelled to be taken), but similar equilibrium biomass levels to that of the higher starting point scenario.

Figures 6 to 8 show the model predicted effective west and south component spawning biomass assuming future recruitment varies about the hockey stick stock recruitment relationships. The directed catch and bycatch is modelled to be taken in >99% of years for the higher starting point scenario (Table 1a), and at a 0.1 or 0.3 movement proportion the effective west component spawning biomass is predicted to be above the 2007 level even at the 5%ile for all catch scenarios. However, if future west to south movement is 0.5 then there is a chance future effective spawning biomass will be below the 2007 level (Figure 8a). For the lower starting point scenario, there are a number of cases for which the full intended directed sardine catch is modelled not to be taken in 2019 (Table 1b). Given these lower catches in 2019 the population is subsequently projected to recover over time to the similar equilibrium level as that achieved from the higher starting point.

Figures 9 to 11 show the model predicted effective west and south component spawning biomass assuming future recruitment is randomly drawn from the most recent 5 years. The directed catch and bycatch is modelled to be taken in >99% of years for the higher starting point scenario (Table 2a). If the future movement proportion is 0.1, the effective west component spawning biomass is predicted to be above the 2007 level at the 5%ile for directed catches up to 20 000t (with a 5000t bycatch) (Figure 9a). However if the future movement proportion is 0.3 the effective west component spawning biomass is predicted to be above the 2007 level only at the 15%ile for directed catches up to 20 000t (with a 5000t bycatch) (Figure 10a). If the future movement proportion is 0.5, even at the 15%ile all effective west component spawning biomass trajectories drop below the 2007 level (Figure 11a). For the lower starting point scenario, there are a number of cases for which the full intended directed sardine catch is not modelled to be taken in 2019 (Table 2b). Given these lower catches in 2019 the population is subsequently projected to recover over time, to the similar equilibrium level as that achieved from the higher starting point, though it should be noted that some of these levels are below the 2007 level.

Results assuming a 10 000t small sardine bycatch are shown in Appendix C.

Summary

In summary, while the alternative movement scenarios influence the short-term rate of increase and long-term equilibrium biomass levels, they have little impact on the level of catches predicted to be possible (according to the selectivity curve assumed) during 2019.

The level of catches predicted to be realised are lower (and less than the intended directed sardine catch at the 30%ile) for the lower 2018 starting point scenario than those achieved for the higher 2018 starting point scenario. Furthermore, if recruitment in November 2018 is of the order of that estimated over the past 5 years, then the predicted realised catch west of Cape Agulhas is lower than that which would realised if recruitment matched the average and associated variability observed over the full historical time period, while the predicted realised catch east of Cape Agulhas is higher than that

which would be realised if recruitment matched the average and associated variability estimated over the full historical time period.

References

Cox S, Gaichas S, Haddon M and Punt AE. 2018. International Review Panel Report for the 2018 International Fisheries Stock Assessment Workshop. International Stock Assessment Workshop, 26-30 November 2018, Cape Town.

de Moor CL. 2019. Assessment of the South African sardine resource using data from 1984-2018: Initial results at the joint posterior mode for the two mixing component hypothesis. DAFF: Branch Fisheries Document FISHERIES/2019/FEB/SWG-PEL/01.

de Moor CL, Bergh M, Butterworth DS, Coetzee JC and van der Lingen CD. 2018. Density dependent movement of South African sardine. DAFF: Branch Fisheries Document FISHERIES/2018/FEB/SWG-PEL/02.

de Moor CL, Butterworth DS and van der Lingen CD. 2017. The quantitative use of parasite data in multistock modelling of South African sardine (*Sardinops sagax*). Canadian Journal of Fisheries and Aquatic Sciences. 74:1895-1903.

Table 1a. The model predicted realised directed sardine catch in **2019** at different percentiles, assuming a 5000t small sardine bycatch, $\mathrm{move}_{y,1} = 0.3$, **and the higher starting point in 2018**. Recruitment varies about a hockey-stick stock recruitment relationship. This indicates cases where there were insufficient sardine in one or more age groups in 2019 for the full catch from that age group to be taken. In the majority of cases the full directed sardine catch is predicted to be taken from 2021 onwards.

Constant TAC input			Realised directed catch in 2019													
Total	West	East	West of Cape Agulhas							East of Cape Agulhas						
			5%ile	10%ile	15%ile	20%ile	30%ile	40%ile	50%ile	5%ile	10%ile	15%ile	20%ile	30%ile	40%ile	50%ile
5000t	3500t	1500t	3500t	3500t	3500t	3500t	3500t	3500t	3500t	1500t	1500t	1500t	1500t	1500t	1500t	1500t
10000t	7000t	3000t	7000t	7000t	7000t	7000t	7000t	7000t	7000t	3000t	3000t	3000t	3000t	3000t	3000t	3000t
20000t	14000t	6000t	14000t	14000t	14000t	14000t	14000t	14000t	14000t	6000t	6000t	6000t	6000t	6000t	6000t	6000t

Table 1b. As per Table 1a, but for the **lower starting point in 2018**.

Constant TAC input			Realised directed catch in 2019													
Total	West	East	West of Cape Agulhas							East of Cape Agulhas						
			5%ile	10%ile	15%ile	20%ile	30%ile	40%ile	50%ile	5%ile	10%ile	15%ile	20%ile	30%ile	40%ile	50%ile
5000t	3500t	1500t	1400t	1900t	2400t	3200t	3500t	3500t	3500t	2t	2t	3t	4t	5t	6t	8t
10000t	7000t	3000t	1400t	1900t	2400t	3200t	4500t	5800t	6900t	2t	2t	3t	4t	5t	6t	8t
20000t	14000t	6000t	1400t	1900t	2400t	3200t	4500t	5800t	6900t	2t	2t	3t	4t	5t	6t	8t

Table 2a. The model predicted realised directed sardine catch in **2019** at different percentiles, assuming a 5000t small sardine bycatch, $\mathrm{move}_{y,1} = 0.3$, **and the higher starting point in 2018**. Recruitment is drawn randomly from the past 5 years. This indicates cases where there were insufficient sardine in one or more age groups in 2019 for the full catch from that age group to be taken. In the majority of cases the full directed sardine catch is predicted to be taken from 2021 onwards.

Constant TAC input			Realised directed catch in 2019													
Total	West	East	West of Cape Agulhas							East of Cape Agulhas						
			5%ile	10%ile	15%ile	20%ile	30%ile	40%ile	50%ile	5%ile	10%ile	15%ile	20%ile	30%ile	40%ile	50%ile
5000t	3500t	1500t	3500t	3500t	3500t	3500t	3500t	3500t	3500t	1500t	1500t	1500t	1500t	1500t	1500t	1500t
10000t	7000t	3000t	7000t	7000t	7000t	7000t	7000t	7000t	7000t	3000t	3000t	3000t	3000t	3000t	3000t	3000t
20000t	14000t	6000t	14000t	14000t	14000t	14000t	14000t	14000t	14000t	6000t	6000t	6000t	6000t	6000t	6000t	6000t

Table 2b. As per Table 2a, but for the **lower starting point in 2018**.

Constant TAC input			Realised directed catch in 2019													
Total	West	East	West of Cape Agulhas							East of Cape Agulhas						
			5%ile	10%ile	15%ile	20%ile	30%ile	40%ile	50%ile	5%ile	10%ile	15%ile	20%ile	30%ile	40%ile	50%ile
5000t	3500t	1500t	900t	900t	1100t	1100t	1200t	3400t	3500t	30t	30t	100t	100t	100t	100t	100t
10000t	7000t	3000t	900t	900t	1100t	1100t	1200t	3400t	4000t	30t	30t	100t	100t	100t	100t	100t
20000t	14000t	6000t	900t	900t	1100t	1100t	1200t	3400t	4000t	30t	30t	100t	100t	100t	100t	100t

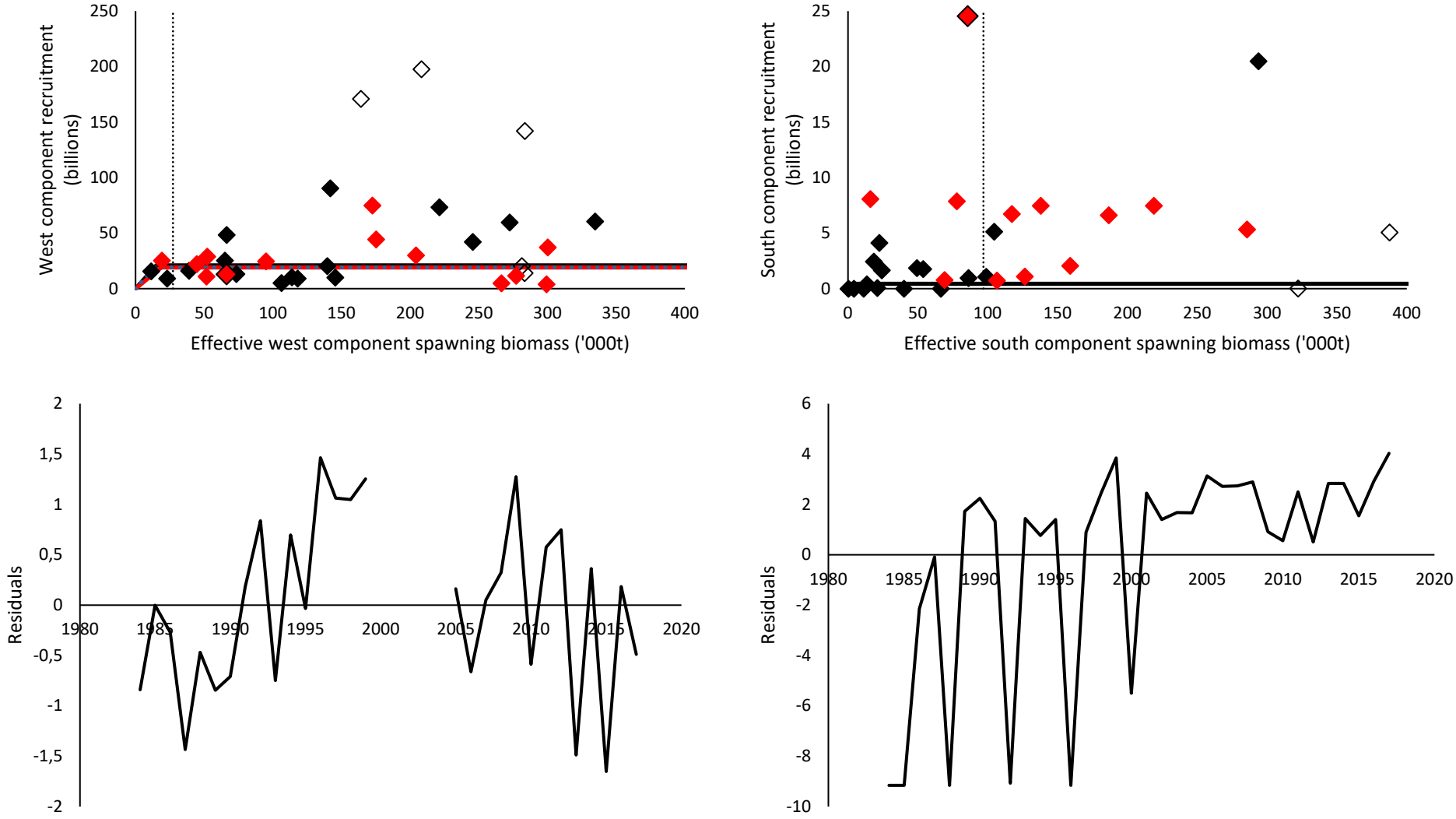

Figure 1. The model predicted recruitment and effective spawning biomass in November between 1984 and 2017 (1984-99 in black diamonds, 2000-04 unfilled diamonds, 2005-17 in red diamonds). Hockey stick stock recruitment curves are fitted to all years. In addition, for the west component, hockey stick stock recruitment curves were also fitted to the 'data' from 2005 to 2017 only and the 'data' corresponding to effective spawning biomasses < 100 000t (the resultant curves a very similar and are indistinguishable on the scale in the above plot). The residuals from the model fit to all years are shown in the lower plots.

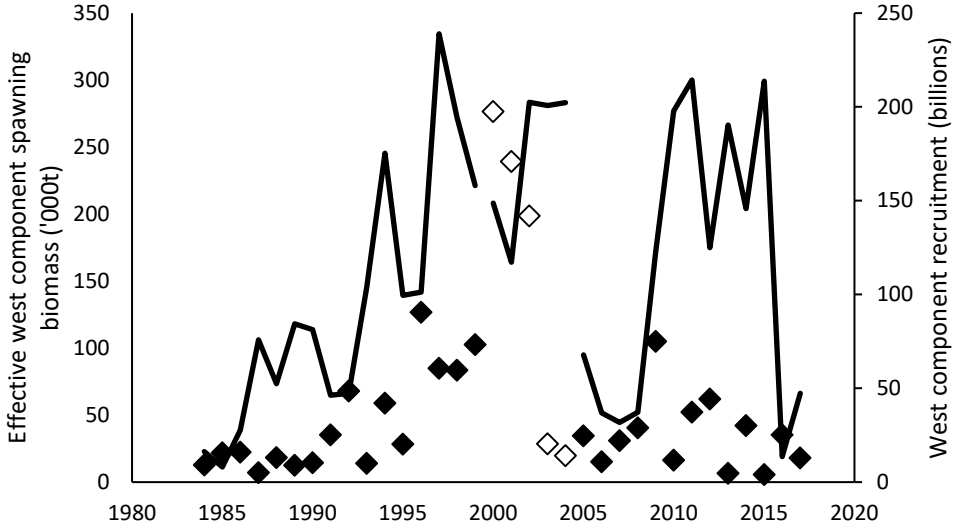

Figure 2. The model predicted west component recruitment (diamonds) and effective spawning biomass (lines) in November between 1984 and 2017.

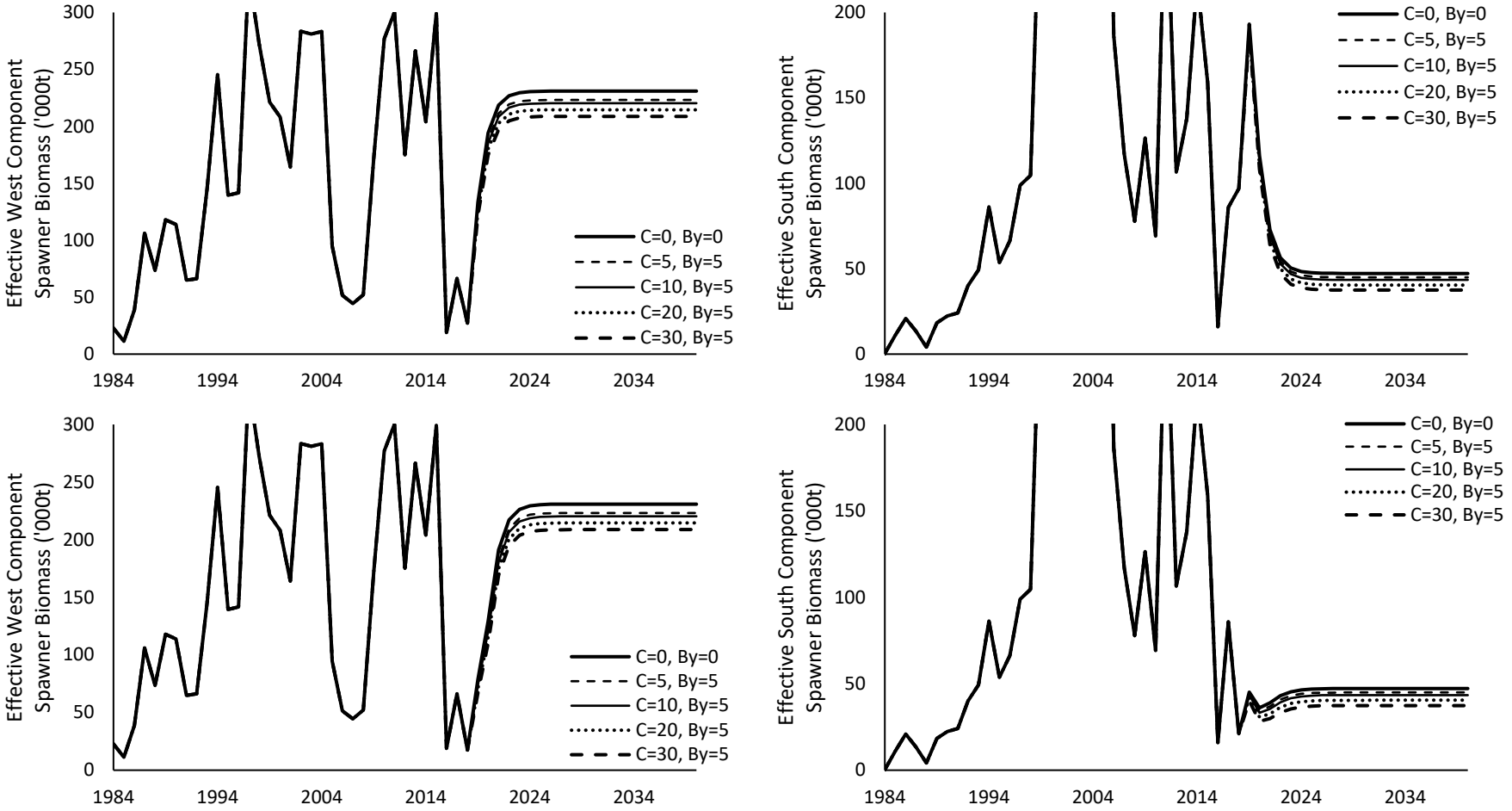

Figure 3. Effective spawning biomass for the (left) west and (right) south components for projections assuming constant directed sardine catches of 0, 5, 10, 20 or 30 000t with a deterministic hockey-stick stock recruitment relationship, and $\mathbf{move}_{y,1} = \mathbf{0.1}$. The upper plots correspond to the higher starting point in 2018 while the lower plots correspond to the lower starting point in 2018. In all cases the full intended catch is modelled to be taken in all years.

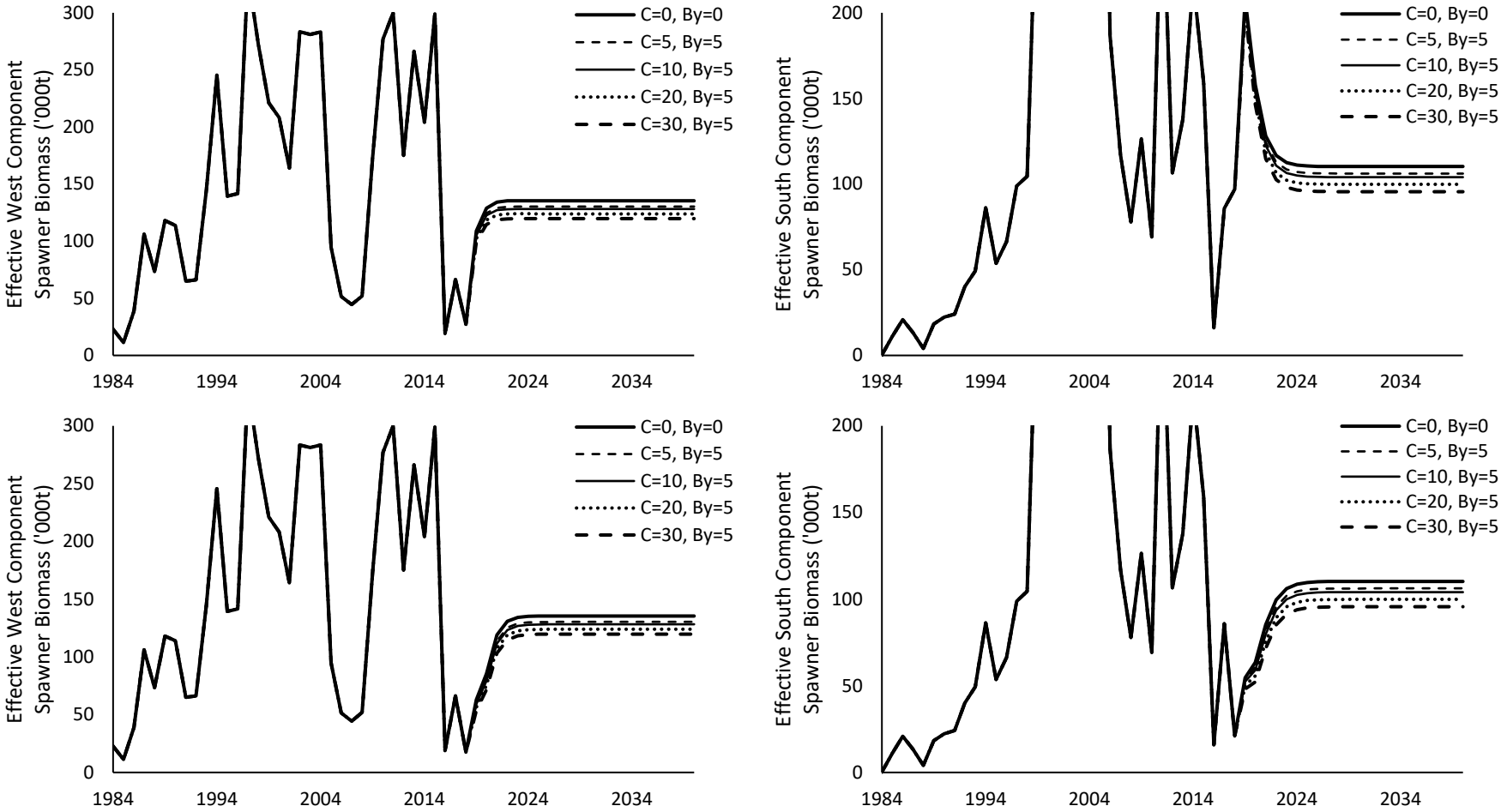

Figure 4. Effective spawning biomass for the (left) west and (right) south components for projections assuming constant directed sardine catches of 0, 5, 10, 20 or 30 000t with a deterministic hockey-stick stock recruitment relationship, and $\mathbf{move}_{\mathbf{y},\mathbf{1}} = \mathbf{0.3}$. The upper plots correspond to the higher starting point in 2018 while the lower plots correspond to the lower starting point in 2018. In all cases the full intended catch is modelled to be taken in all years.

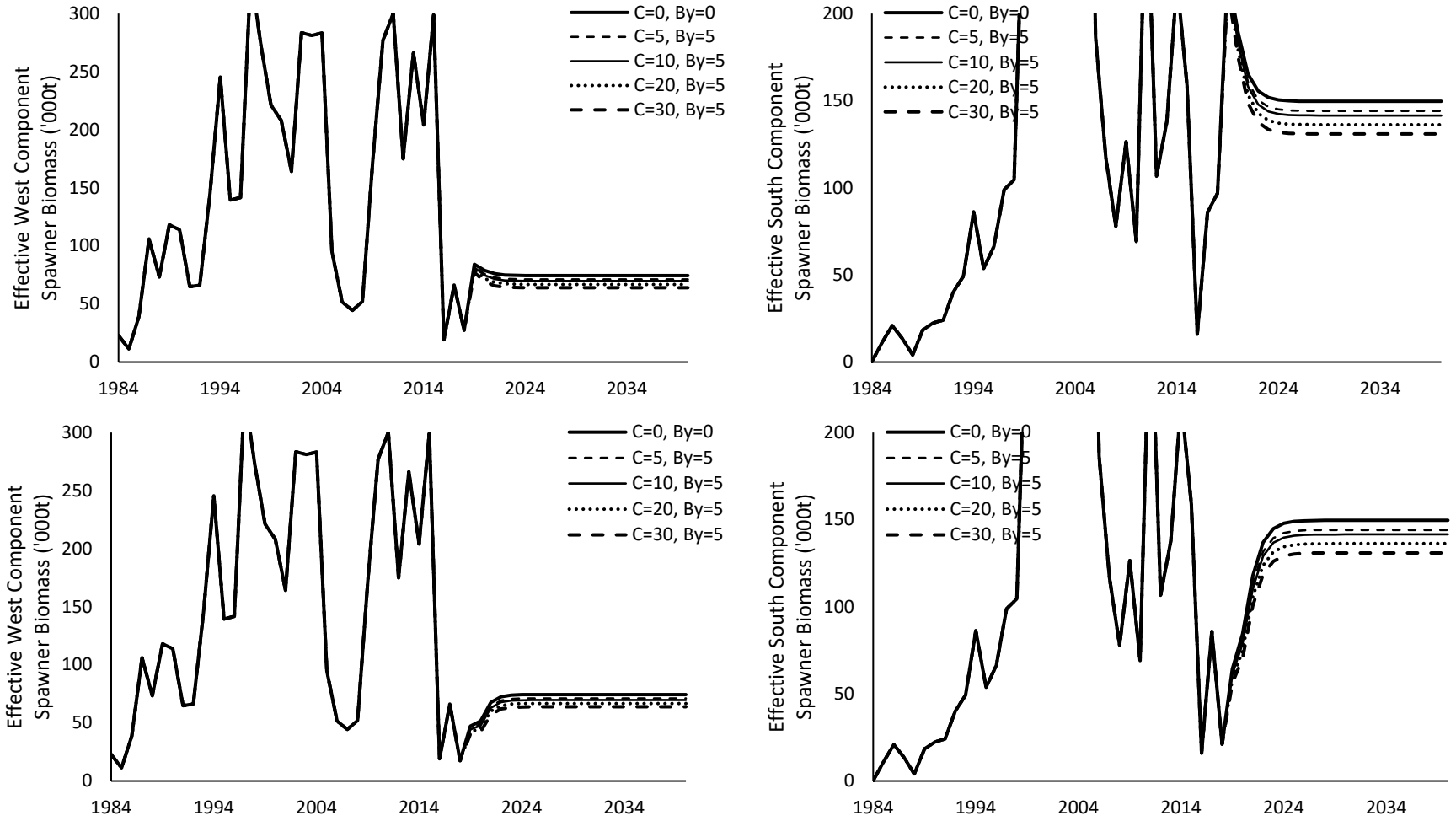

Figure 5. Effective spawning biomass for the (left) west and (right) south components for projections assuming constant directed sardine catches of 0, 5, 10, 20 or 30 000t with a deterministic hockey-stick stock recruitment relationship, and $\mathbf{move}_{y,1} = \mathbf{0.5}$. The upper plots correspond to the higher starting point in 2018 while the lower plots correspond to the lower starting point in 2018. In all cases the full intended catch is modelled to be taken in all years.

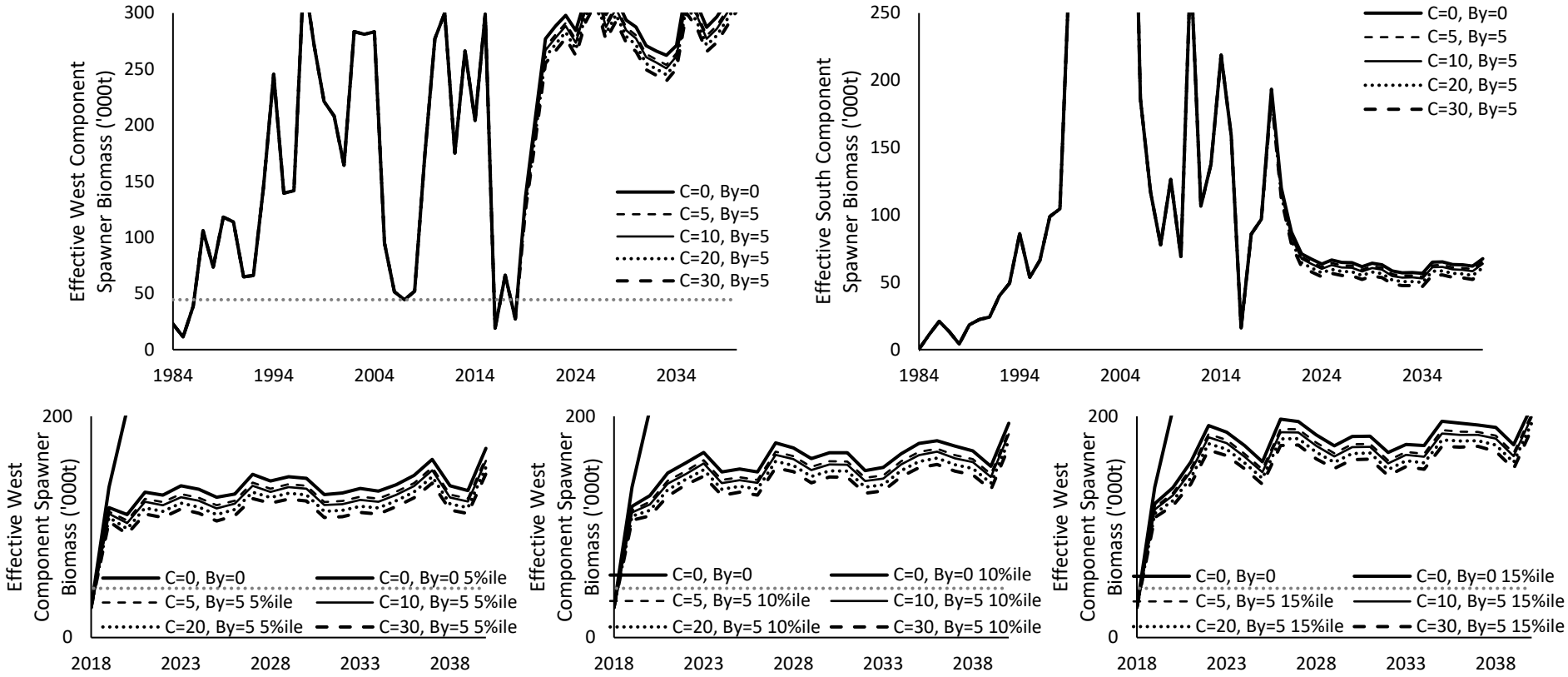

Figure 6a. Effective spawning biomass for the (left) west and (right) south components for projections assuming constant directed sardine catches of 0, 5, 10, 20 or 30 000t with variability about a hockey-stick stock recruitment relationship, and $\mathbf{move}_{\mathbf{y,1}} = \mathbf{0.1}$. The upper plots show the median while the lower plots show the 5, 10 and 15%ile for the west component over a narrower range on both axes. These plots correspond to the higher starting point in 2018. The grey dotted line indicates the risk threshold of the 2007 effective west component spawning biomass.

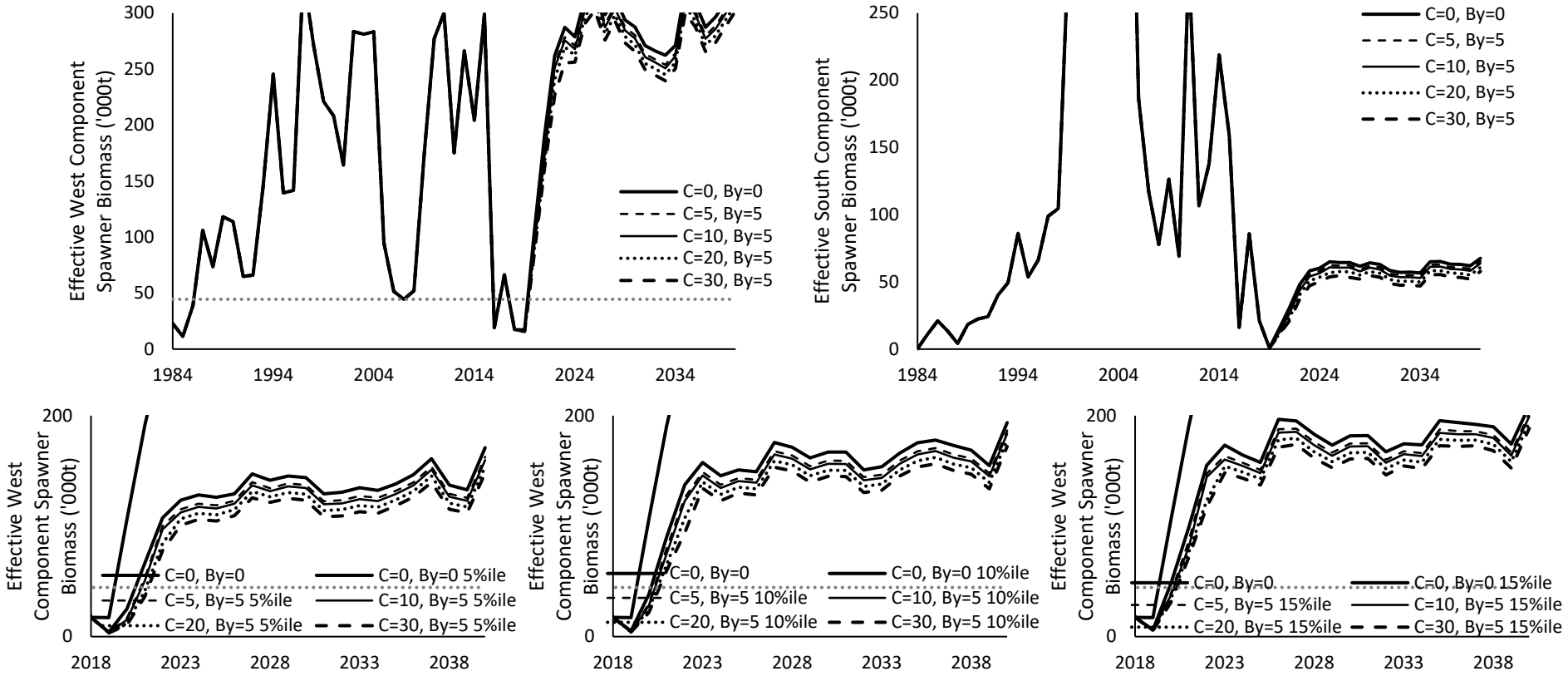

Figure 6b. As per Figure 7a, but with lower starting point in 2018.

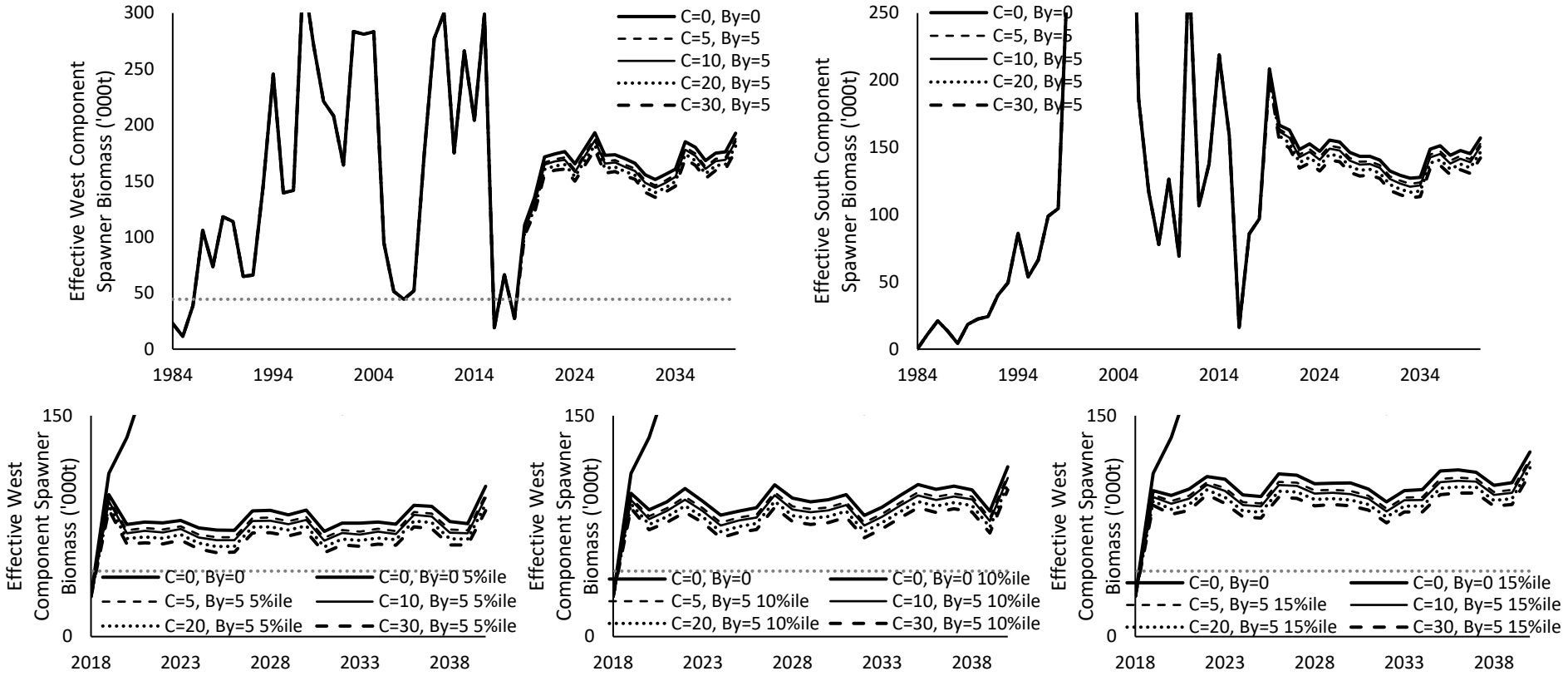

Figure 7a. Effective spawning biomass for the (left) west and (right) south components for projections assuming constant directed sardine catches of 0, 5, 10, 20 or 30 000t with variability about a hockey-stick stock recruitment relationship, and $\mathbf{move}_{y,1} = \mathbf{0.3}$. The upper plots show the median while the lower plots show the 5, 10 and 15%ile for the west component over a narrower range on both axes. These plots correspond to the higher starting point in 2018. The grey dotted line indicates the risk threshold of the 2007 effective west component spawning biomass.

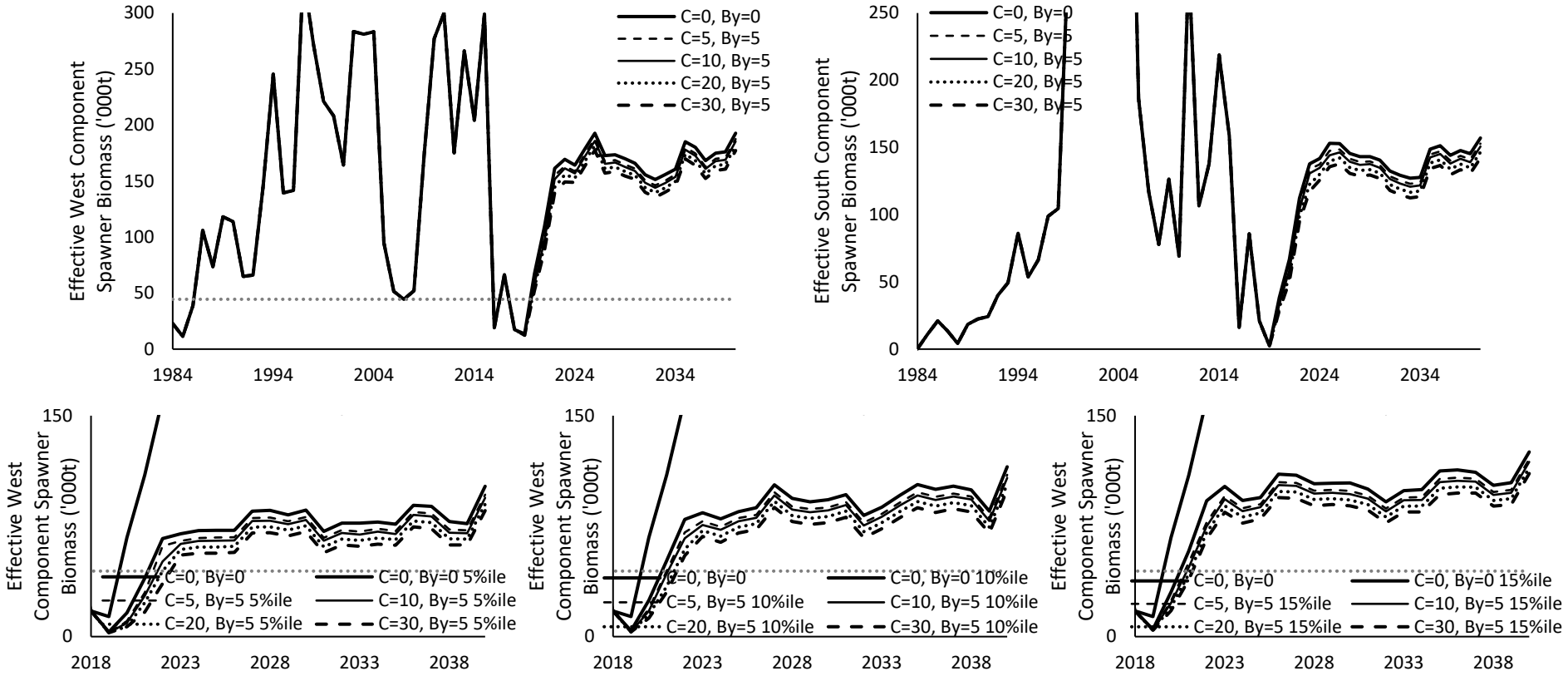

Figure 7b. As per Figure 7a, but with lower starting point in 2018.

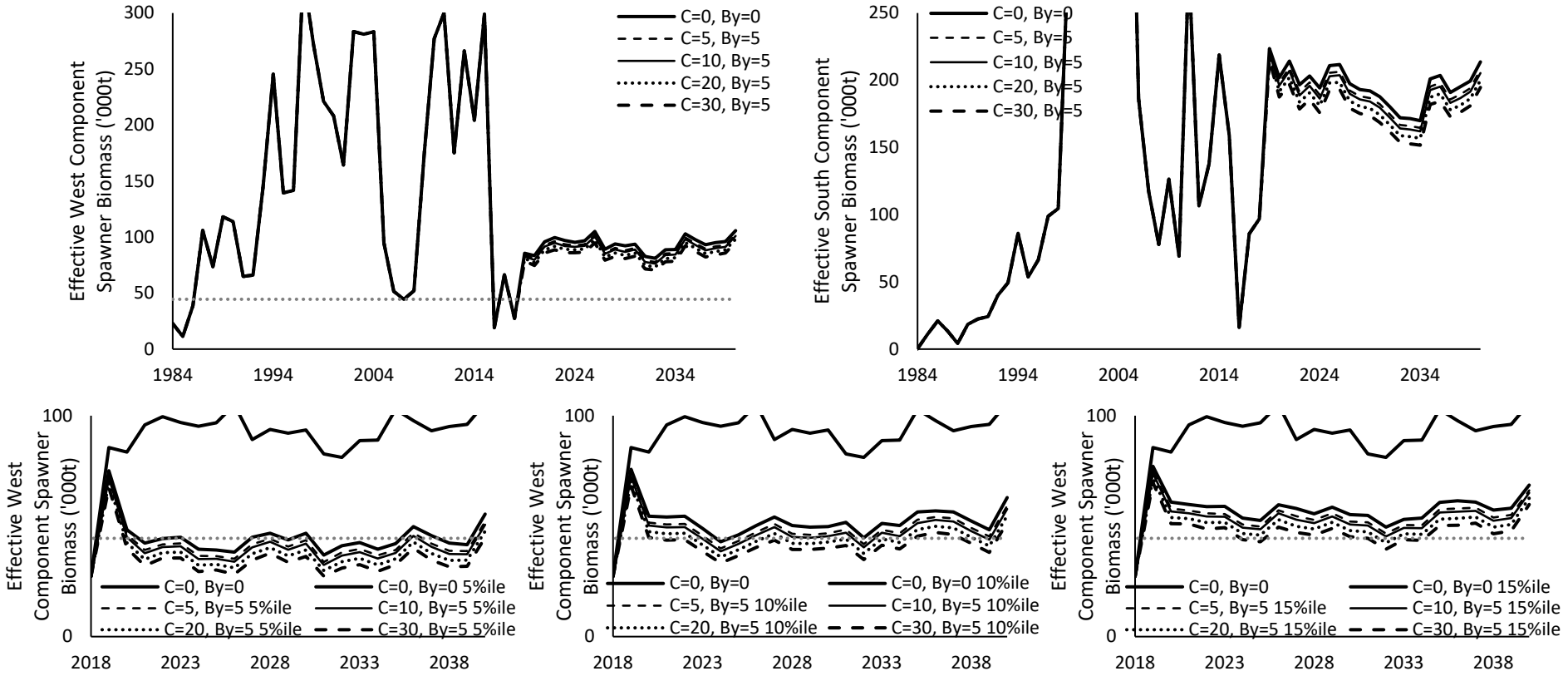

Figure 8a. Effective spawning biomass for the (left) west and (right) south components for projections assuming constant directed sardine catches of 0, 5, 10, 20 or 30 000t with variability about a hockey-stick stock recruitment relationship, and $\mathbf{move}_{y,1} = \mathbf{0.5}$. The upper plots show the median while the lower plots show the 5, 10 and 15%ile for the west component over a narrower range on both axes. These plots correspond to the higher starting point in 2018. The grey dotted line indicates the risk threshold of the 2007 effective west component spawning biomass.

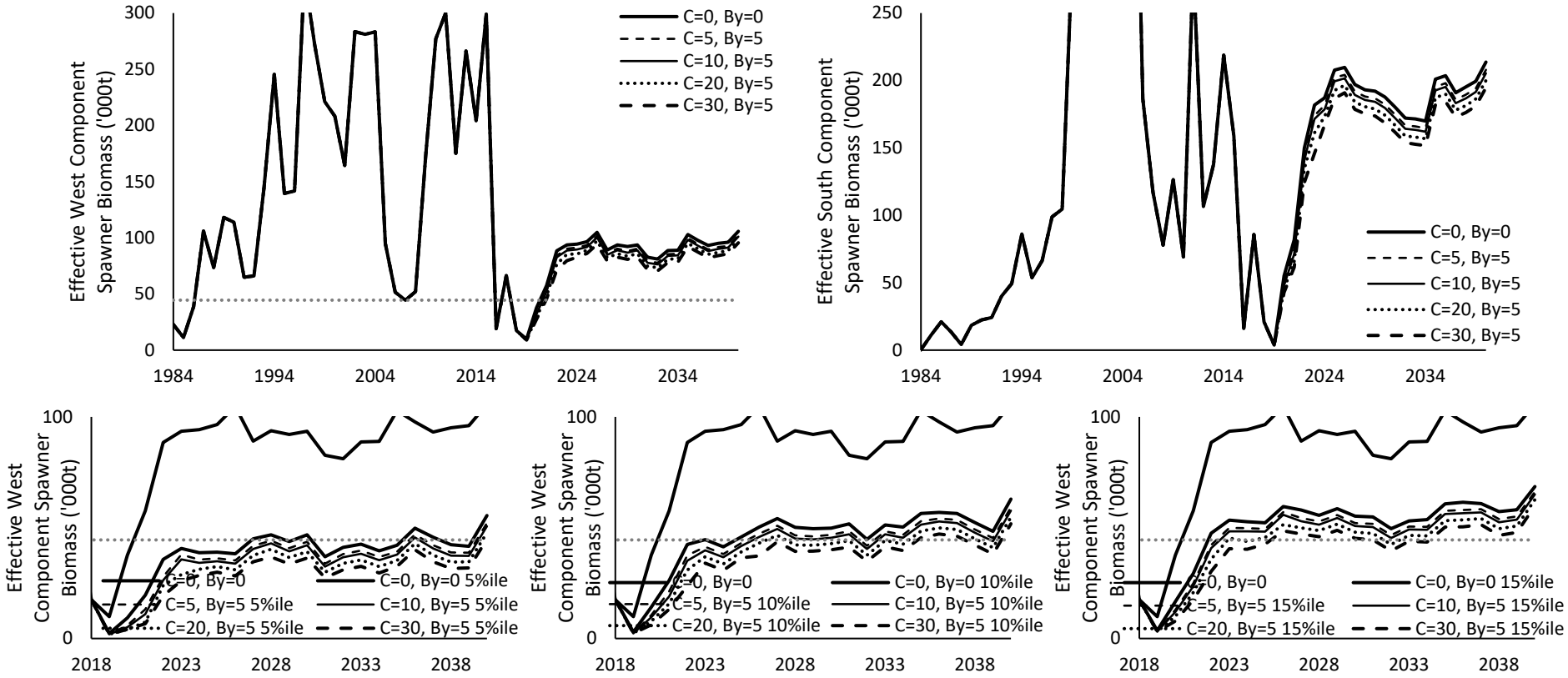

Figure 8b. As per Figure 8a, but with lower starting point in 2018.

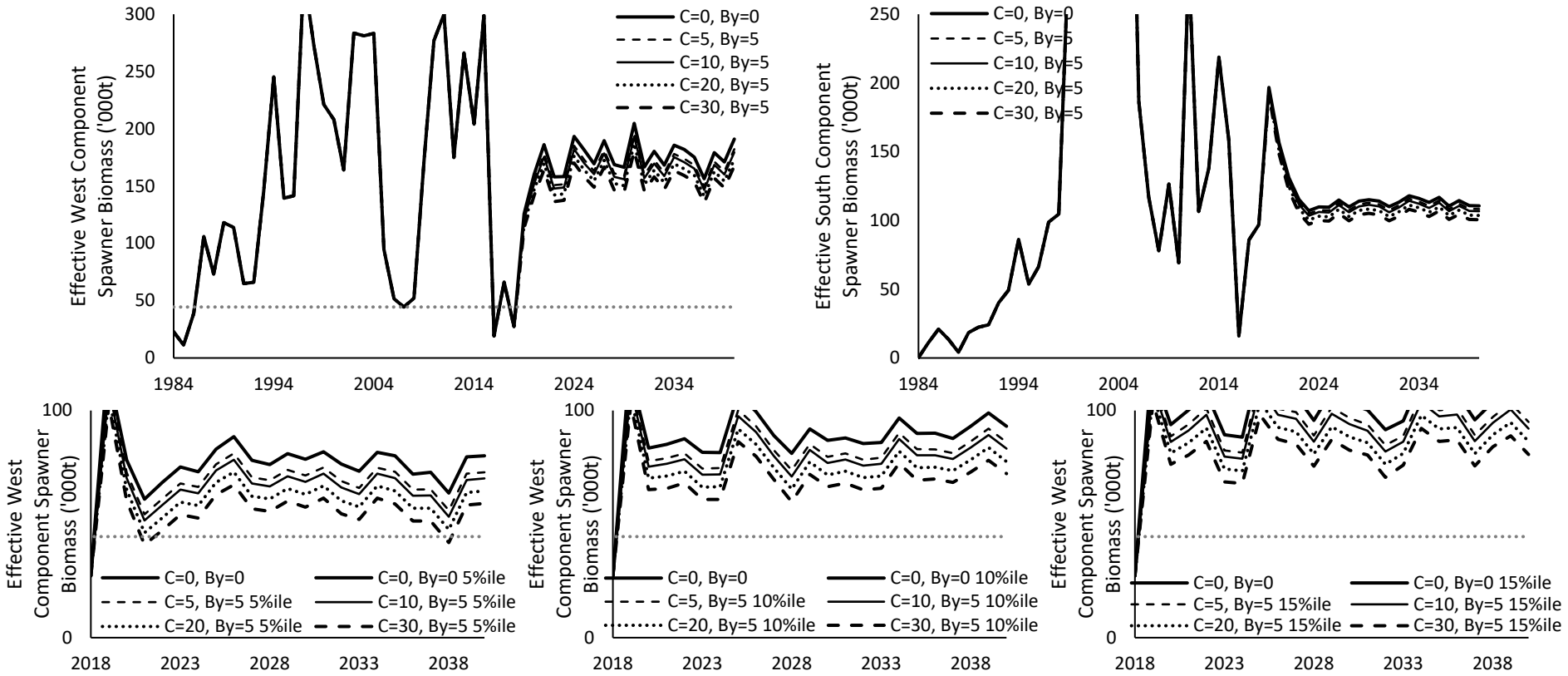

Figure 9a. Effective spawning biomass for the (left) west and (right) south components for projections assuming constant directed sardine catches of 0, 5, 10, 20 or 30 000t with recruitment drawn randomly from the past 5 years, and $\mathbf{move}_{y,1} = \mathbf{0.1}$. The upper plots show the median while the lower plots show the 5, 10 and 15%ile for the west component over a narrower range on both axes. These plots correspond to the higher starting point in 2018. The grey dotted line indicates the risk threshold of the 2007 effective west component spawning biomass.

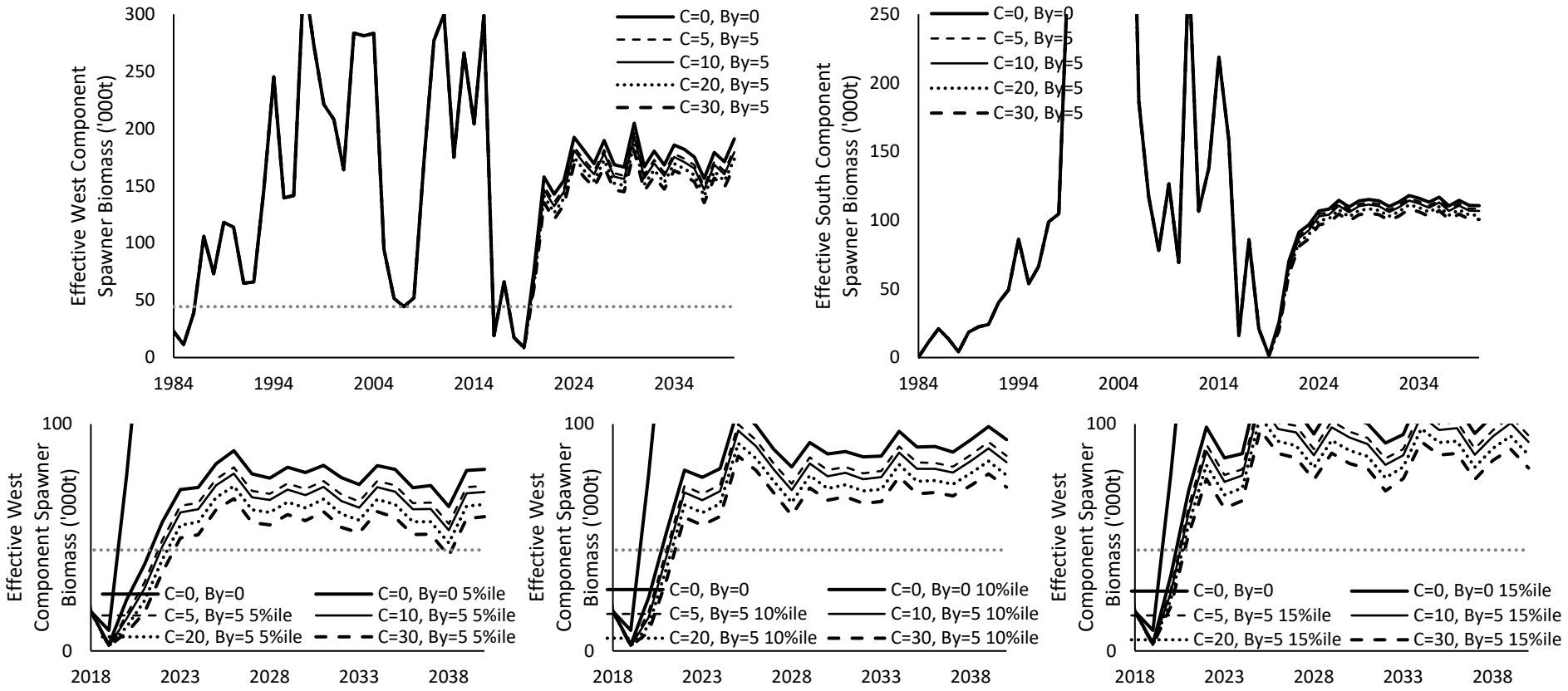

Figure 9b. As per Figure 9a, but with lower starting point in 2018.

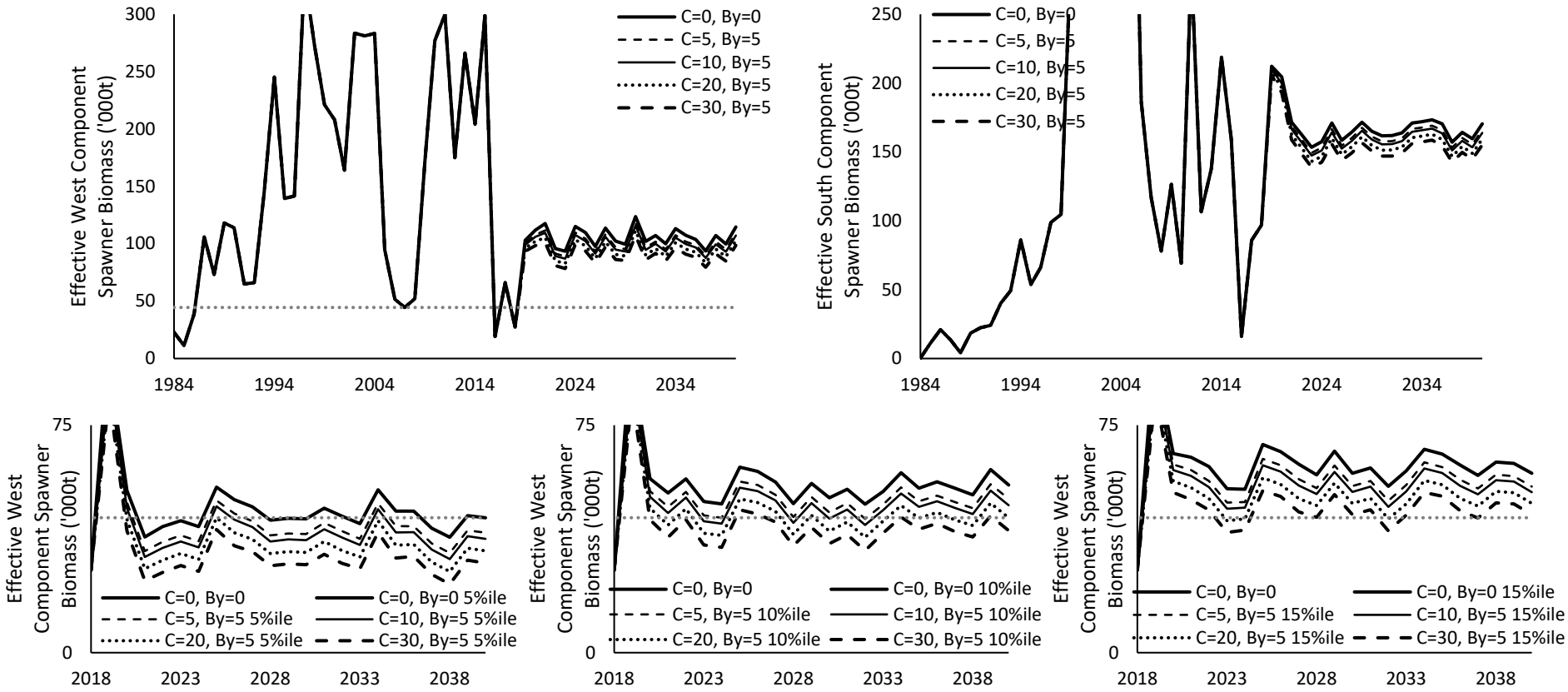

Figure 10a. Effective spawning biomass for the (left) west and (right) south components for projections assuming constant directed sardine catches of 0, 5, 10, 20 or 30 000t with recruitment drawn randomly from the past 5 years, and $\mathbf{move}_{y,1} = \mathbf{0.3}$. The upper plots show the median while the lower plots show the 5, 10 and 15%ile for the west component over a narrower range on both axes. These plots correspond to the higher starting point in 2018. The grey dotted line indicates the risk threshold of the 2007 effective west component spawning biomass.

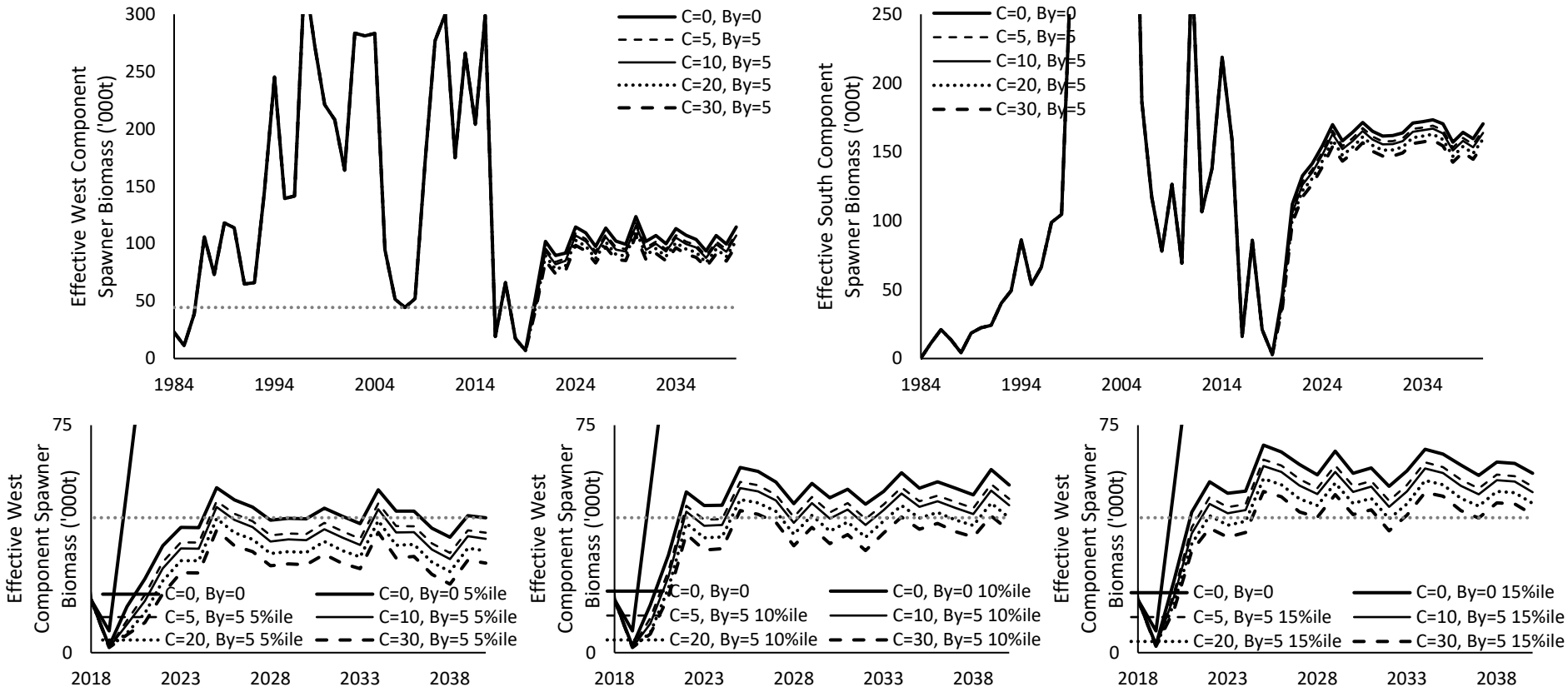

Figure 10b. As per Figure 10a, but with lower starting point in 2018.

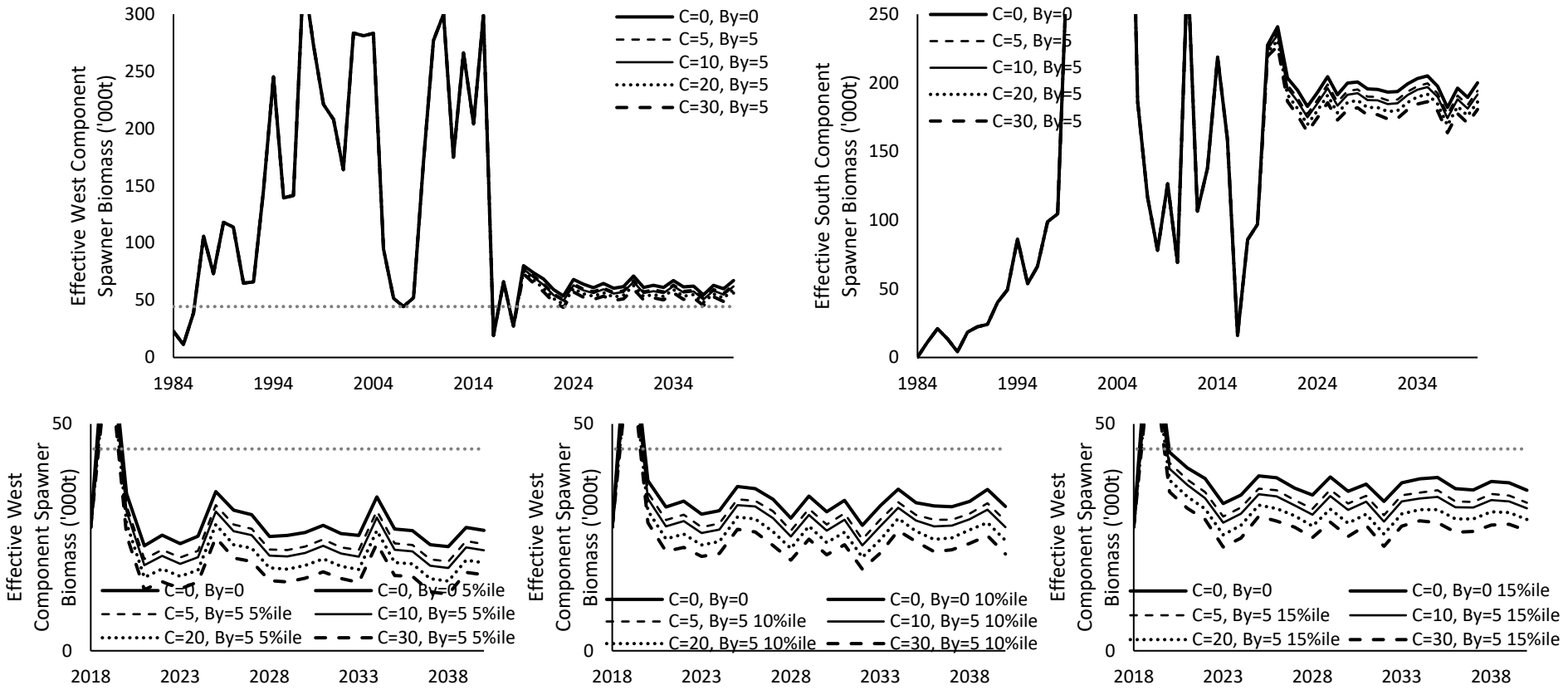

Figure 11a. Effective spawning biomass for the (left) west and (right) south components for projections assuming constant directed sardine catches of 0, 5, 10, 20 or 30 000t with recruitment drawn randomly from the past 5 years, and $\mathbf{move}_{y,1} = \mathbf{0.5}$. The upper plots show the median while the lower plots show the 5, 10 and 15%ile for the west component over a narrower range on both axes. These plots correspond to the higher starting point in 2018. The grey dotted line indicates the risk threshold of the 2007 effective west component spawning biomass.

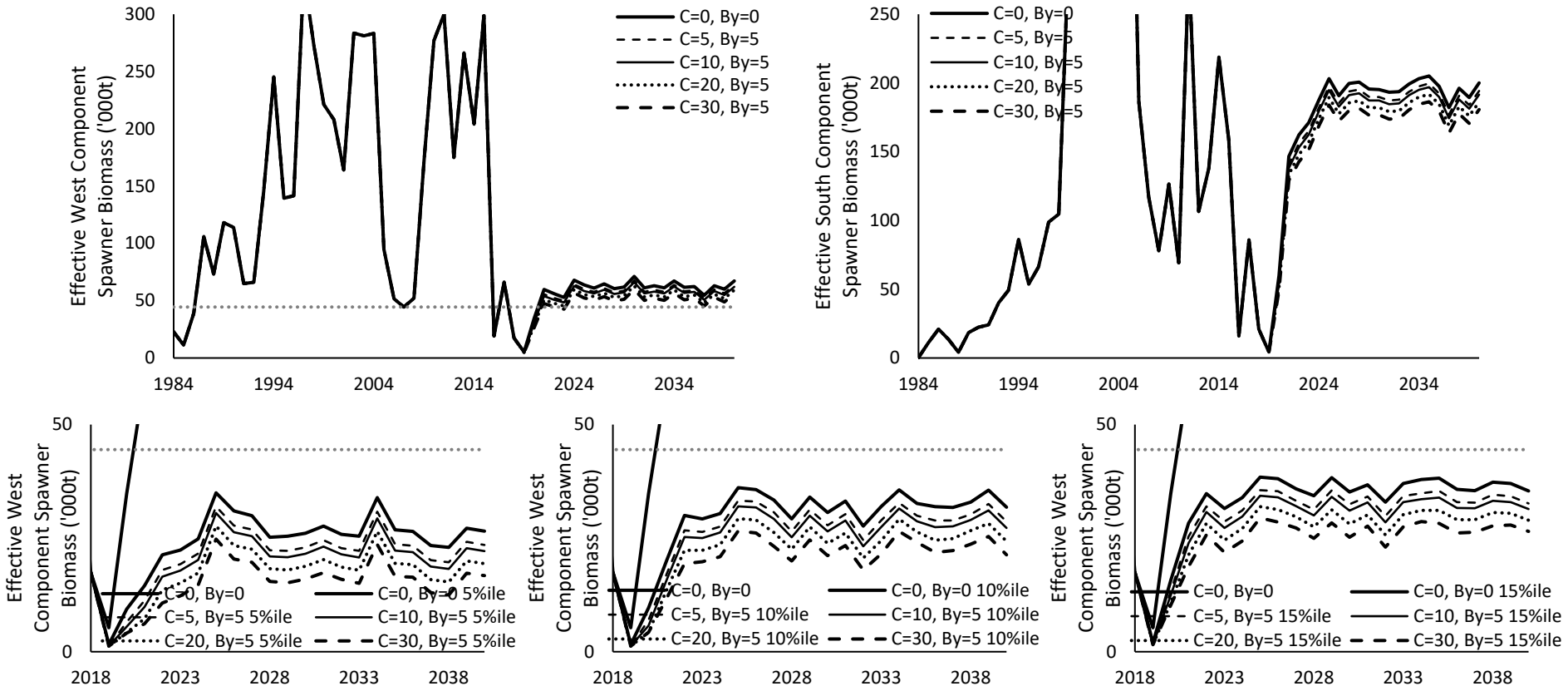

Figure 11b. As per Figure 11a, but with lower starting point in 2018.

Appendix A: Projections using constant catch assumptions

The projections are run from November $y_1 = 2018$ to November $y_n = 2040$. The notation from Appendix A and Tables A1 and A2 of de Moor (2018) remain the same. The following assumptions are made:

- The numbers-at-age are calculated as follows:

$$N^{S*}_{j,p,y,a} = \left(N^{S}_{j,p,y-1,a-1} e^{-M^{S}_{y,a-1}/2} - C^{S}_{j,p,y,a-1}\right) e^{-M^{S}_{y,a-1}/2} \qquad p = I, NI, y_1 \le y \le y_n, 1 \le a \le 5^{+} \tag{1}$$

$$N^{S*}_{j,p,y,5^{+}} = \left(N^{S}_{j,p,y-1,4} e^{-M^{S}_{y,4}/2} - C^{S}_{j,p,y,4}\right) e^{-M^{S}_{y,4}/2} + \left(N^{S}_{j,p,y-1,5^{+}} e^{-M^{S}_{y,5^{+}}/2} - C^{S}_{j,p,y,5^{+}}\right) e^{-M^{S}_{y,5^{+}}/2}$$

$$p = I, NI, y_1 \le y \le y_n \tag{2}$$

and

$$\mathrm{N}^{\mathrm{S}}_{\mathrm{W,p,y,a}} = \left(1 - \mathrm{move}_{\mathrm{y,a}}\right)\mathrm{N}^{\mathrm{S**}}_{\mathrm{W,p,y,a}} \qquad p = I, NI, y_1 \le y \le y_n, 1 \le a \le 5^{+}$$

$$\mathrm{N}^{\mathrm{S}}_{\mathrm{S,p,y,a}} = \mathrm{N}^{\mathrm{S**}}_{\mathrm{S,p,y,a}} + \mathrm{move}_{\mathrm{y,a}}\mathrm{N}^{\mathrm{S**}}_{\mathrm{W,p,y,a}} \qquad p = I, NI, y_1 \le y \le y_n, 1 \le a \le 5^{+} \tag{3}$$

- Future infection is assumed to be zero (this is inconsequential to projections)
- Future movement of 1-year olds is assumed to be either $\mathrm{move}_{\mathrm{y,1}}$ =0.1., $\mathrm{move}_{\mathrm{y,1}}$ =0.3 or $\mathrm{move}_{\mathrm{y,1}}$ =0.5.
- Future recruitment is according to the hockey stick stock recruitment function, estimated after conditioning of the model on historical data (see Appendix B)

$$N^{S}_{j,p,y,a=0} = \begin{cases} a^{S}_{j} e^{\varepsilon^{S}_{j,y}} & if\ p = NI\ and\ SSB^{eff,S}_{j,y} \ge b^{S}_{j} \\ a^{S}_{j} \frac{SSB^{eff,S}_{j,y}}{b^{S}_{j}} e^{\varepsilon^{S}_{j,y}} & if\ p = NI\ and\ SSB^{eff,S}_{j,y} < b^{S}_{j} \\ 0 & if\ p = I \end{cases} \qquad y_1 \le y \le y_n \tag{4}$$

- Natural mortality is assumed to be time-invariant: $M^{S}_{y,a=0} = \bar{M}^{S}_{ju}$ and $M^{S}_{y,a=1+} = \bar{M}^{S}_{ad}$
- No allowance is made for early/late recruitment in future years, i.e. $\varepsilon^{t}_{y} = 0$ in equation (A8).
- Growth curves at the mid-point of each quarter (equation A17) and therefore the quarterly commercial selectivity-at-age functions (equation A16) are the same for all future years.
- Growth curves in November (equation A7) are thus also the same for all future years.
- Future annual selectivity-at-age is assumed to be time-invariant and averaged over all quarters of the most recent commercial selectivity-at-length estimated from 2002-2018 (note growth curves are time-invariant in future years):

$$S^{S}_{j,a} = 0.25 \sum_{q=1}^{4} \sum_{l=2.5^{-}}^{24^{+}} A^{com}_{j,2019,q,a,l} S_{j,2018,q,l} = 0.25 \quad 0 \le a \le 5^{+} \tag{5}$$

- The numbers-at-length are calculated according to equations (A5) and (A6).
- The same maturity-at-length relationship, based on that corresponding to the period 1965-1975, is assumed from 2004 onwards, for all projected years.
- The November biomass, spawner biomass and effective spawner biomass are calculated according to equations (A11) to (A13). However, the weight-at-length in these equations is assumed to be the average of the most recent 10 years, i.e. $w^{S}_{j,y,l} = \frac{1}{10} \sum_{y=2009}^{2018} w^{S}_{j,y,l}$, $2.5^{-} cm \le l \le 24^{+} cm$. (6)
- Catch weight-at-age is taken to be the average of the weight-at-age in November immediately before and after the pulse fishery is assumed, i.e.

$$w^{catch}_{j,a} = 0.5\left(w^{S}_{j,a} + w^{S}_{j,a+1}\right) \qquad 0 \le a \le 4$$

$$w_{j,5^+}^{catch} = w_{j,5^+}^{S} \quad (7)$$

where

$$w_{j,a}^{S} = \sum_{l=2.5^-}^{l=24^+} A_{j,2019,a,l}^{sur} w_{j,2019,l}^{S} \quad (8)$$

- Catch is assumed to be taken in a single pulse, mid-way through the year. Bycatch is calculated as:

$$C_{j,p,y,a}^{bycatch} = \frac{Bycatch}{\sum_{a=0}^{1}\sum_{p=I,NI} N_{j,p,y-1,a}^{S} e^{-M_{y,a}^{S}/2} w_{j,a}^{catch}} \times N_{j,p,y-1,a}^{S} e^{-M_{y,a}^{S}/2} \leq N_{j,p,y-1,a}^{S} e^{-M_{y,a}^{S}/2}$$

and directed catch (taken to include large sardine bycatch) is calculated as:

$$C_{j,p,y,a}^{dir} = \frac{Directed+Large\ Bycatch}{\sum_{a=0}^{5^+}\sum_{p=I,NI}\left(N_{j,p,y-1,a}^{S} e^{-M_{y,a}^{S}/2} - C_{j,p,y,a}^{bycatch}\right) S_{j,a}^{S} w_{j,a}^{catch}} \times \left(N_{j,p,y-1,a}^{S} e^{-M_{y,a}^{S}/2} - C_{j,p,y,a}^{bycatch}\right) S_{j,a}^{S} \leq$$

$$\left(N_{j,p,y-1,a}^{S} e^{-M_{y,a}^{S}/2} - C_{j,p,y,a}^{bycatch}\right) S_{j,a}^{S}$$

$$C_{j,p,y,a}^{S} = C_{j,p,y,a}^{bycatch} + C_{j,p,y,a}^{dir} \qquad p = I, NI, y > y_n, 1 \leq q \leq 4, 0 \leq a \leq 5^+ \quad (9)$$

Appendix B: Estimation of hockey-stick stock recruitment relationships

November recruitment to stock j in year y is calculated as follows for all years except the pulse west component years of 2000-2004:

$$N_{j,y}^{pred} = \begin{cases} a_j^S & if\ SSB_{j,y}^{eff,S} \geq b_j^S \\ a_j^S \frac{SSB_{j,y}^{eff,S}}{b_j^S} & if\ SSB_{j,y}^{eff,S} < b_j^S \end{cases}$$

The parameters a_j^S, the maximum recruitment of component j in the hockey stick model, and b_j^S, the effective spawner biomass below which the expectation for recruitment is reduced below the maximum for component j are estimated by minimising

$$-lnL = \sum_{y=1984}^{2017} \sum_j \left[ln\left(\sigma_j^S\right) + \frac{\left(ln\left(N_{j,NI,y,0}^S\right) - ln\left(N_{j,y}^{pred}\right)\right)^2}{2\left(\sigma_j^S\right)^2} \right]$$

where $\sigma_W^S = \frac{1}{29}\sum_y \left(ln\left(N_{W,NI,y,0}^S\right) - ln\left(N_{W,y}^{pred}\right)\right)^2$ and $\sigma_S^S = \frac{1}{29}\sum_y \left(ln\left(N_{S,NI,y,0}^S\right) - ln\left(N_{S,y}^{pred}\right)\right)^2$.

Appendix B: Further results, assuming 10 000t small sardine bycatch

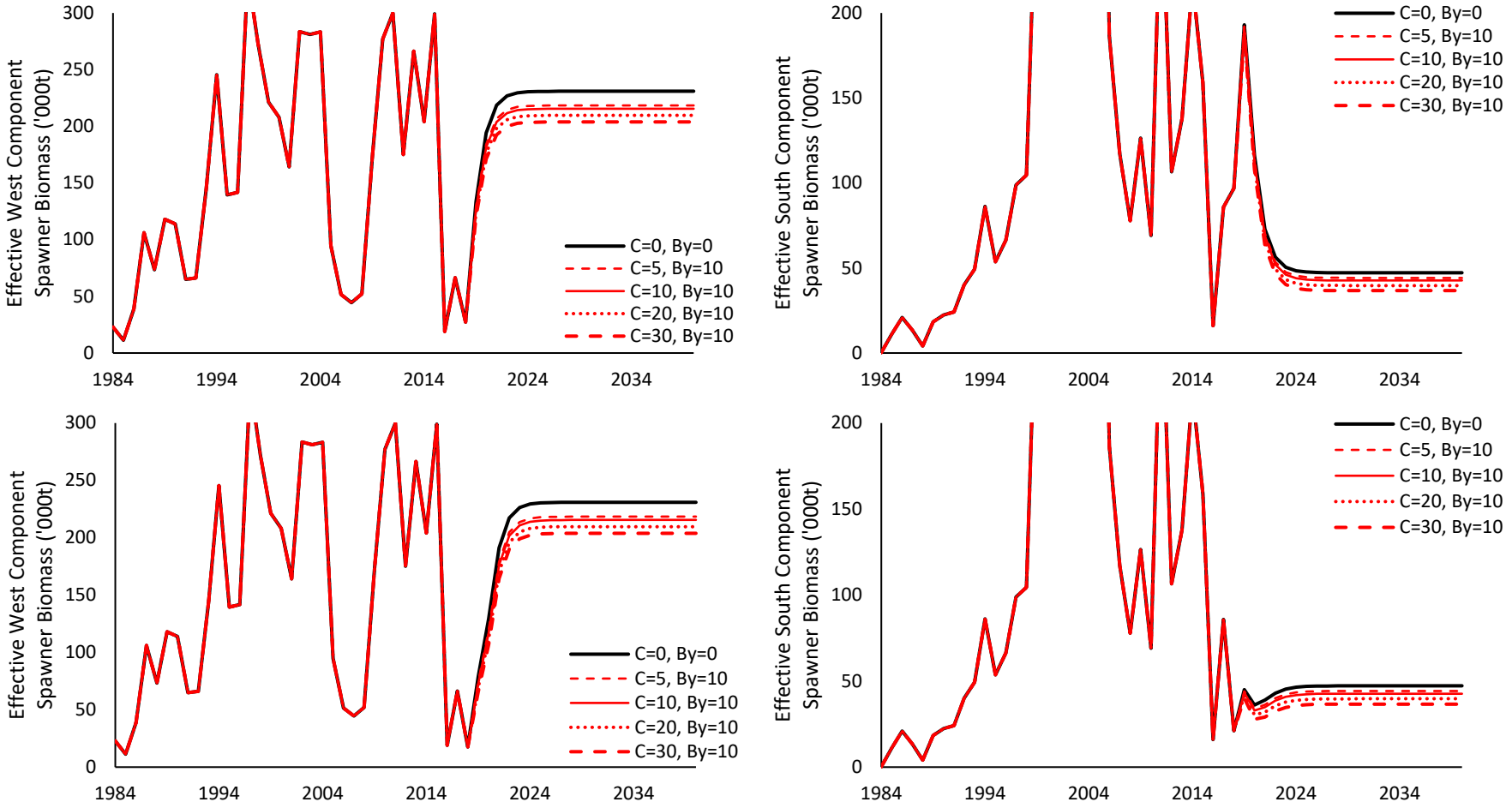

Figure B1. Effective spawning biomass for the (left) west and (right) south components for projections assuming constant directed sardine catches of 0, 5, 10, 20 or 30 000t with a deterministic hockey-stick stock recruitment relationship, and $\mathbf{move}_{y,1} = \mathbf{0.1}$. The upper plots correspond to the higher starting point in 2018 while the lower plots correspond to the lower starting point in 2018. In all cases the full intended catch is modelled to be taken in all years.

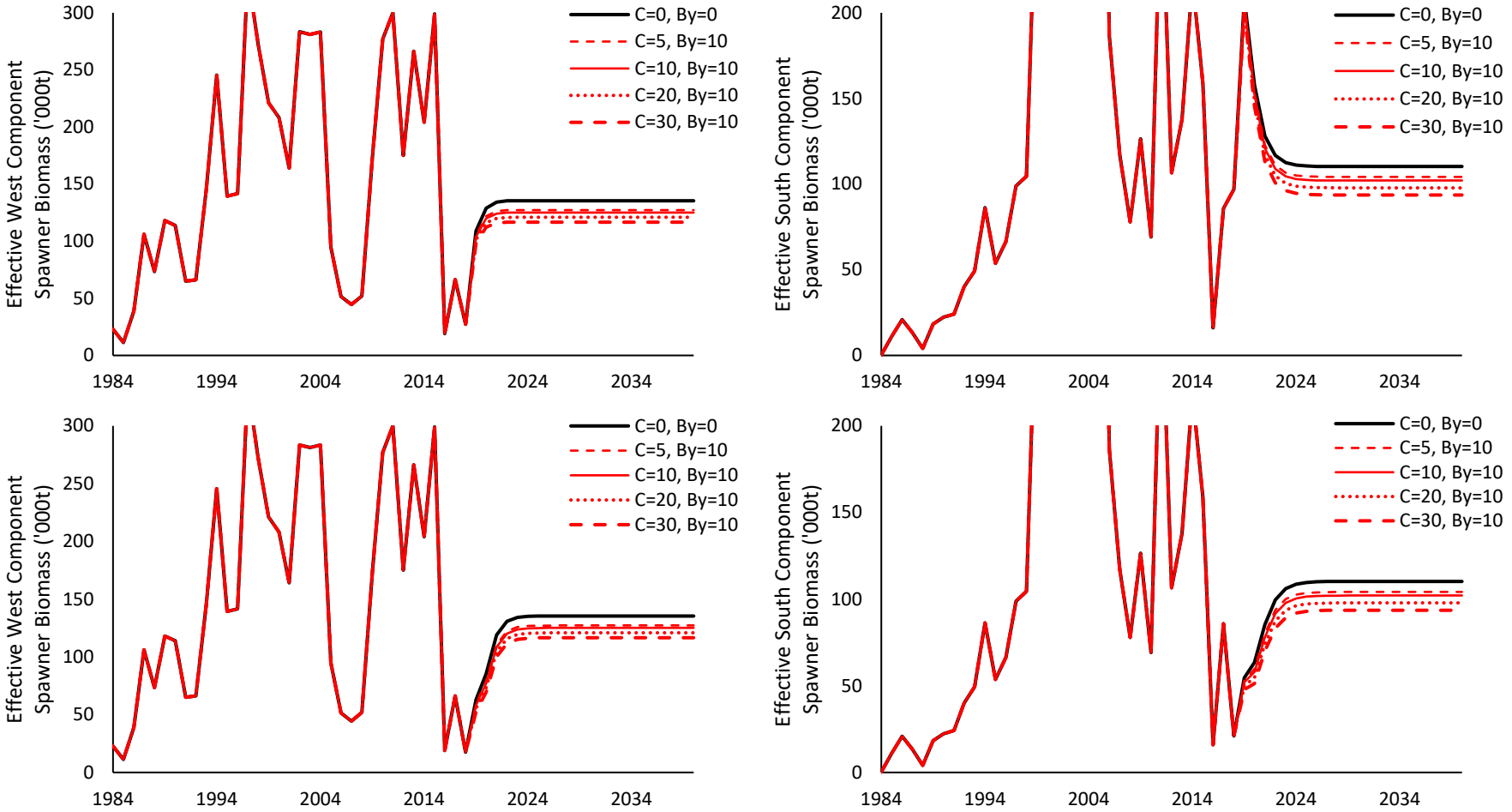

Figure B2. Effective spawning biomass for the (left) west and (right) south components for projections assuming constant directed sardine catches of 0, 5, 10, 20 or 30 000t with a deterministic hockey-stick stock recruitment relationship, and $\mathbf{move}_{y,1} = \mathbf{0.3}$. The upper plots correspond to the higher starting point in 2018 while the lower plots correspond to the lower starting point in 2018. In all cases the full intended catch is modelled to be taken in all years.

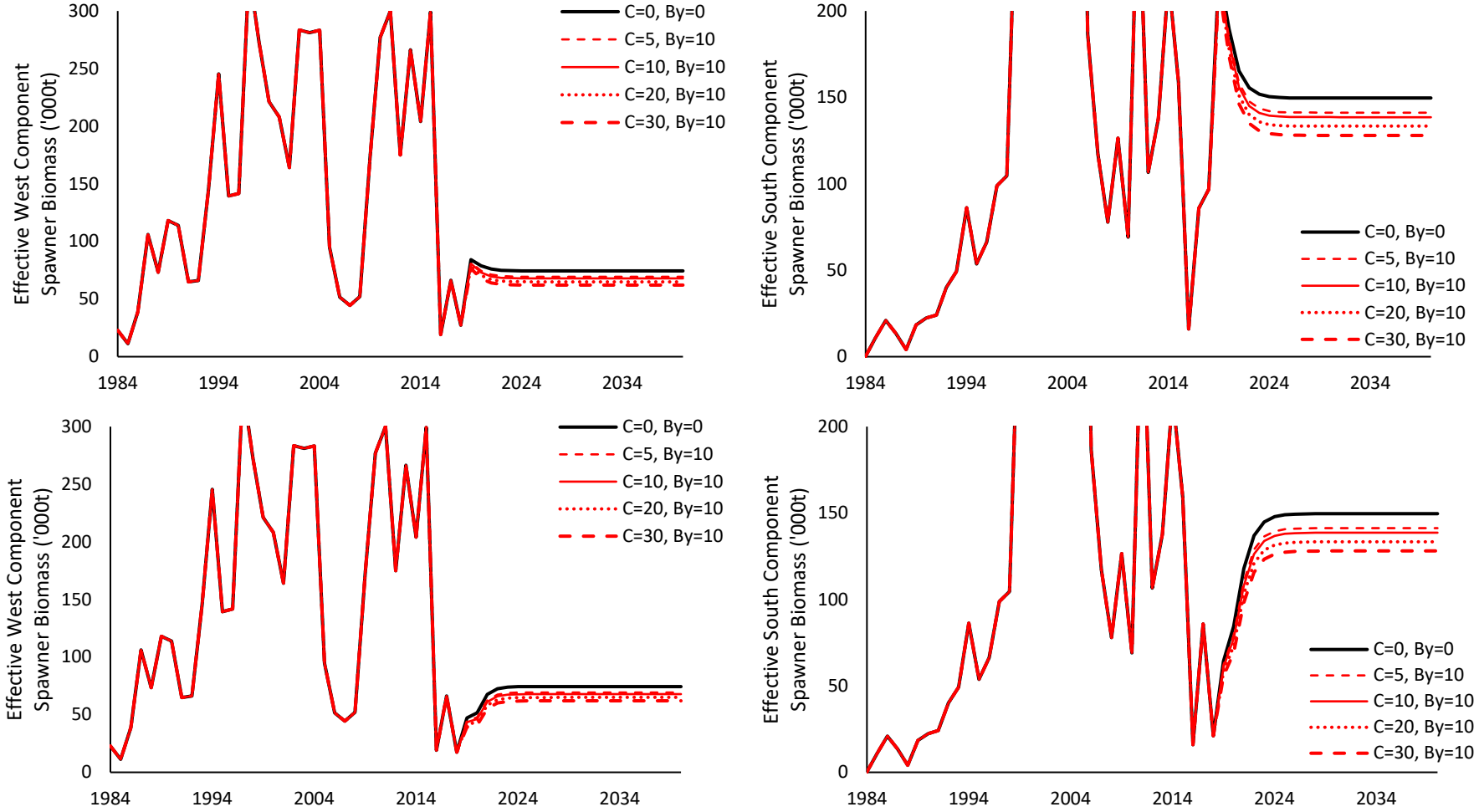

Figure B3. Effective spawning biomass for the (left) west and (right) south components for projections assuming constant directed sardine catches of 0, 5, 10, 20 or 30 000t with a deterministic hockey-stick stock recruitment relationship, and $\mathbf{move}_{y,1} = \mathbf{0.5}$. The upper plots correspond to the higher starting point in 2018 while the lower plots correspond to the lower starting point in 2018. In all cases the full intended catch is modelled to be taken in all years.

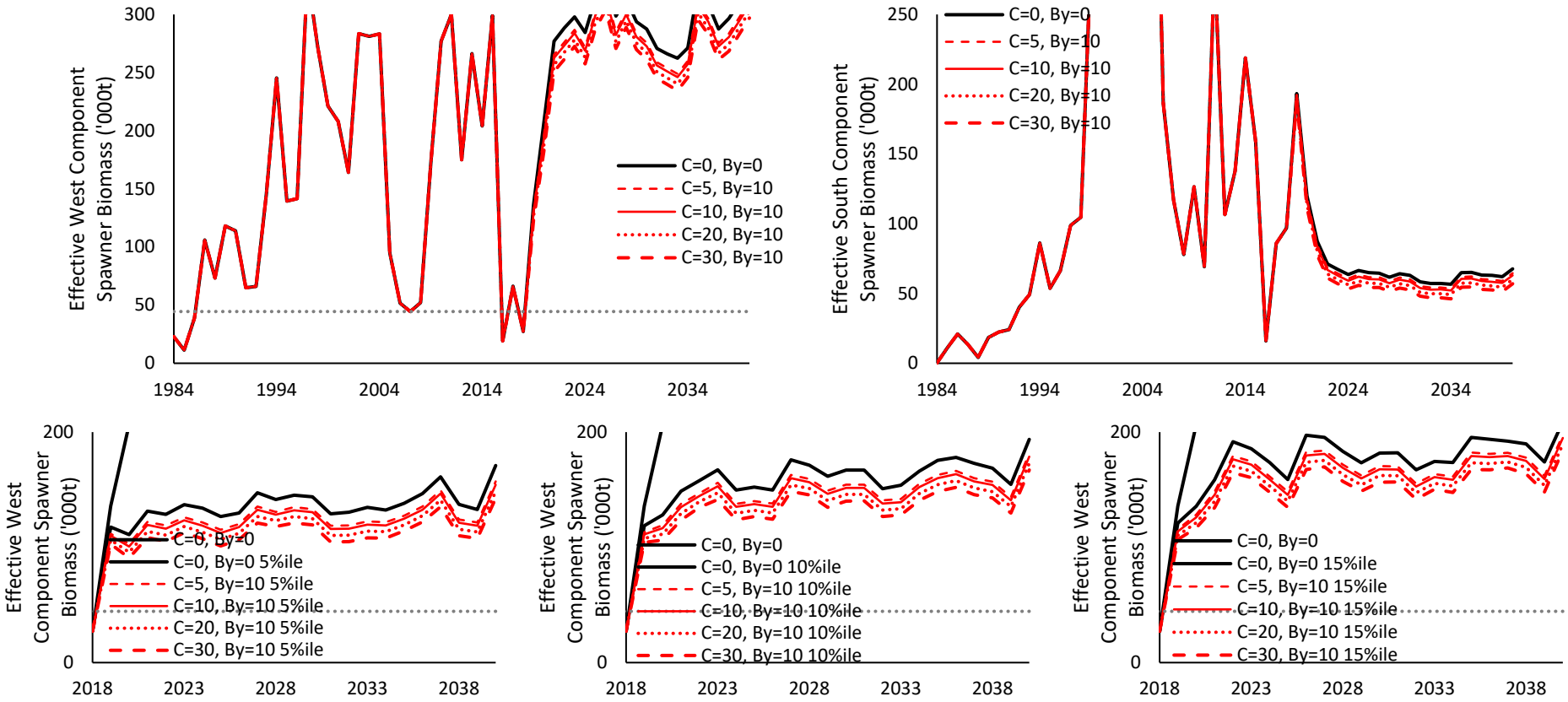

Figure B4a. Effective spawning biomass for the (left) west and (right) south components for projections assuming constant directed sardine catches of 0, 5, 10, 20 or 30 000t with variability about a hockey-stick stock recruitment relationship, and $\mathbf{move}_{y,1} = \mathbf{0.1}$. The upper plots show the median while the lower plots show the 5, 10 and 15%ile for the west component over a narrower range on both axes. These plots correspond to the higher starting point in 2018. The grey dotted line indicates the risk threshold of the 2007 effective west component spawning biomass.

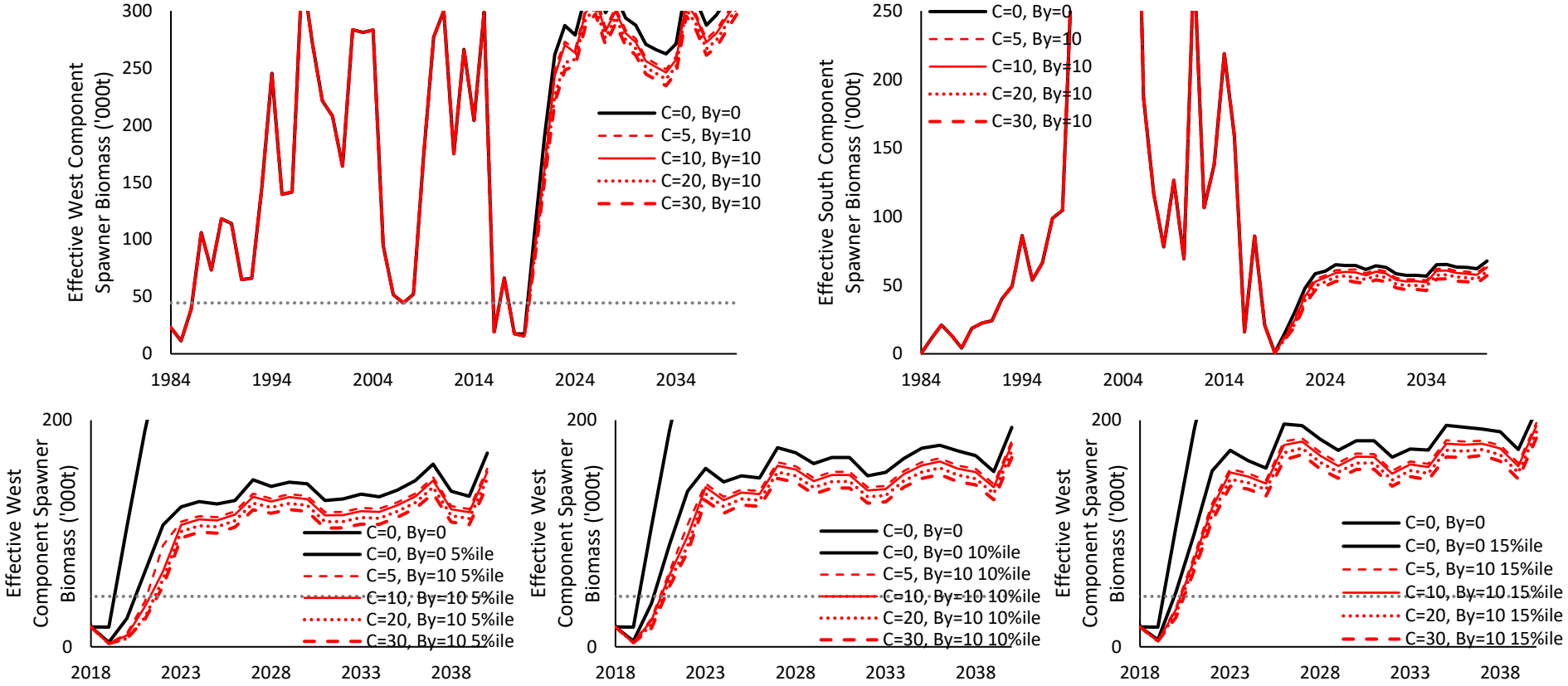

Figure B4b. As per Figure 7a, but with lower starting point in 2018.

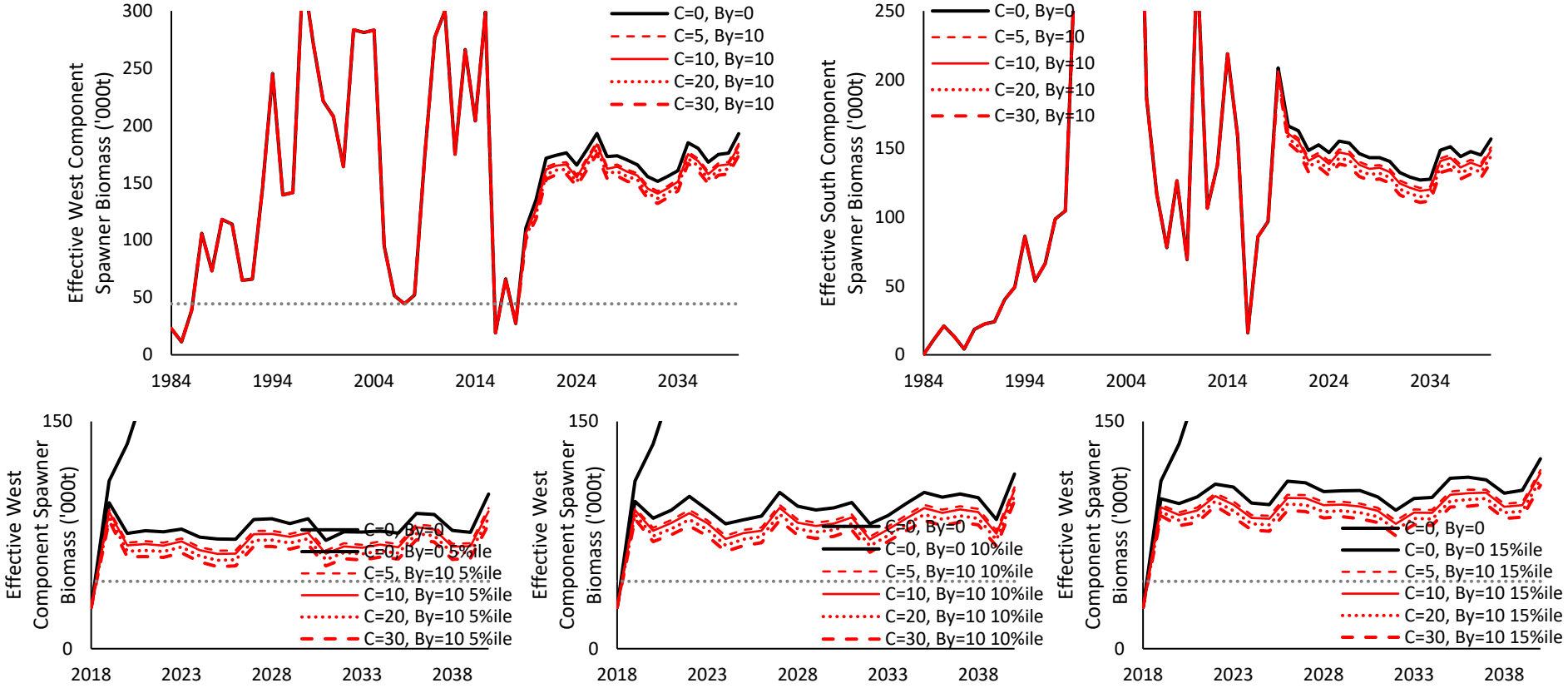

Figure B5a. Effective spawning biomass for the (left) west and (right) south components for projections assuming constant directed sardine catches of 0, 5, 10, 20 or 30 000t with variability about a hockey-stick stock recruitment relationship, and $\mathbf{move}_{y,1} = \mathbf{0.3}$. The upper plots show the median while the lower plots show the 5, 10 and 15%ile for the west component over a narrower range on both axes. These plots correspond to the higher starting point in 2018. The grey dotted line indicates the risk threshold of the 2007 effective west component spawning biomass.

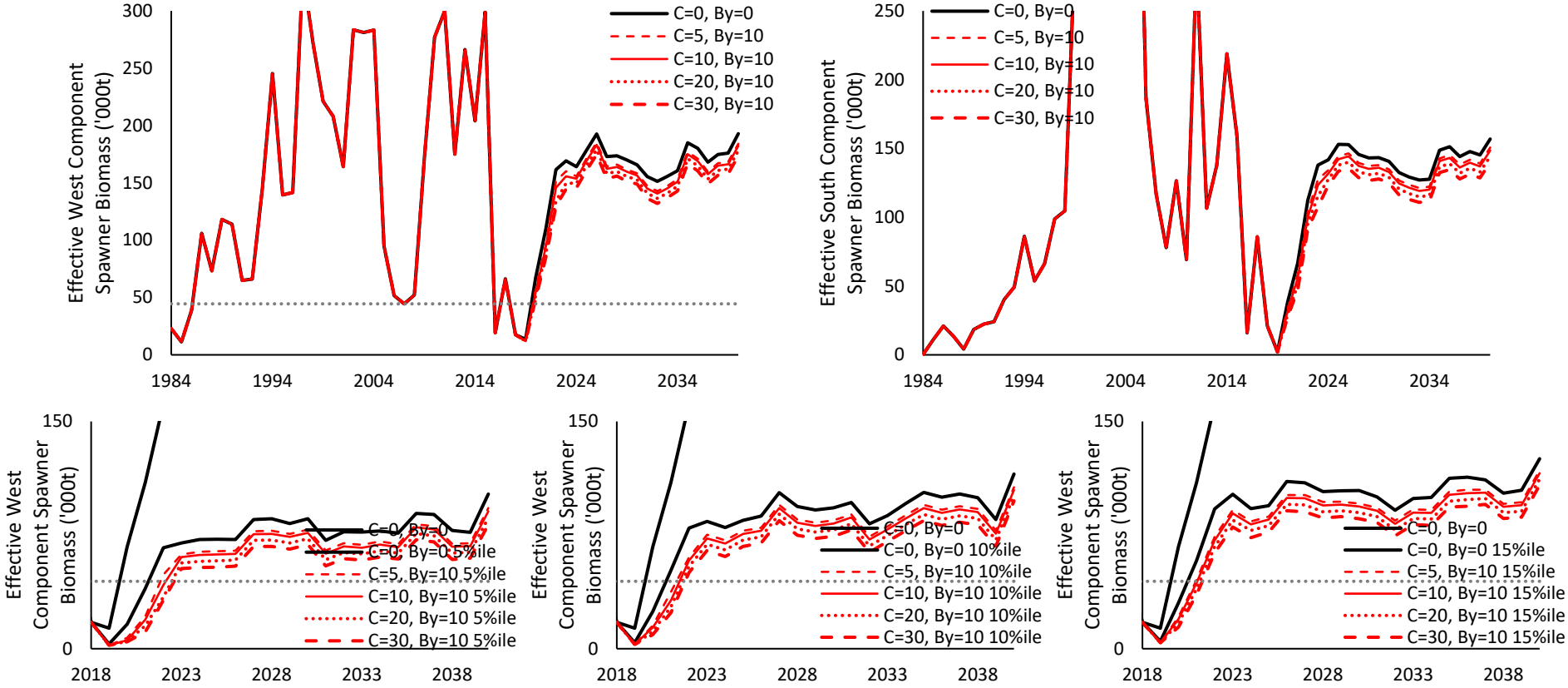

Figure B5b. As per Figure 7a, but with lower starting point in 2018.

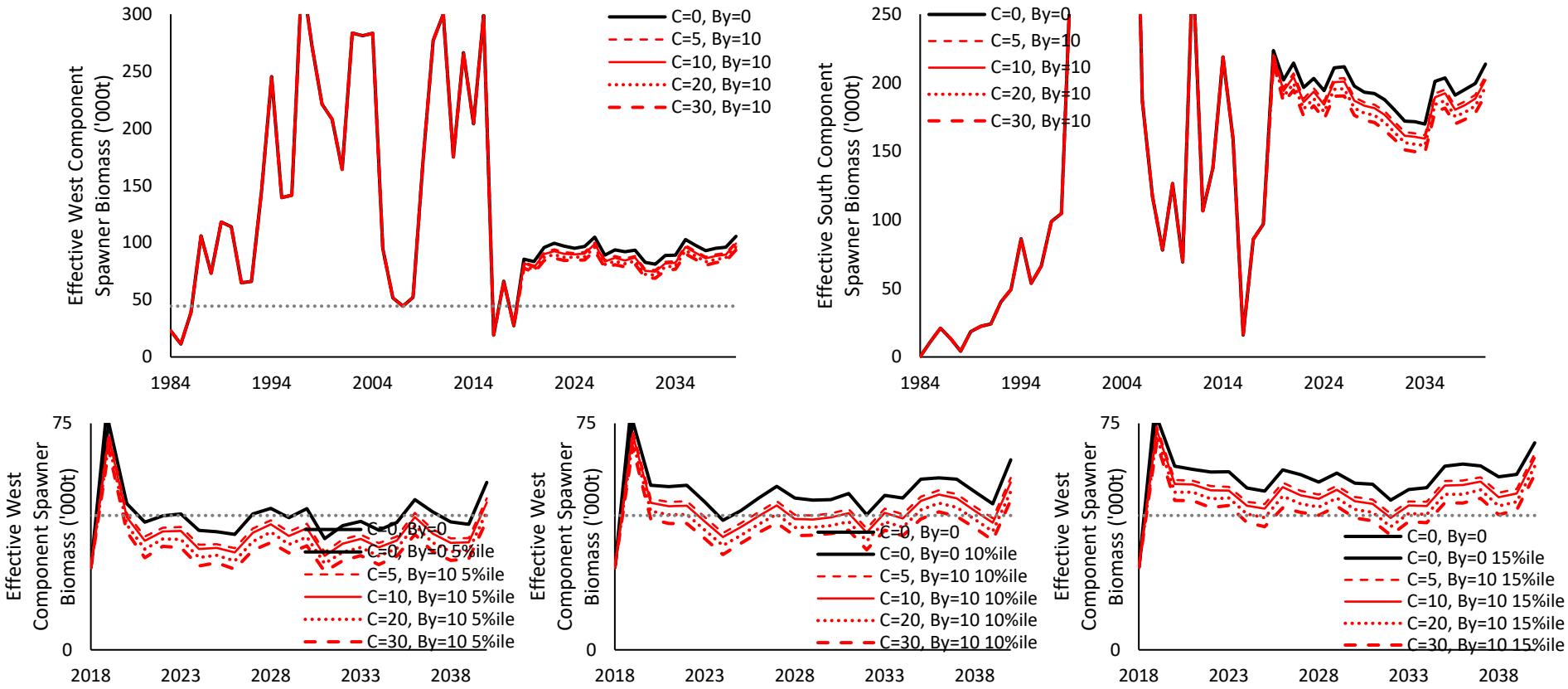

Figure B6a. Effective spawning biomass for the (left) west and (right) south components for projections assuming constant directed sardine catches of 0, 5, 10, 20 or 30 000t with variability about a hockey-stick stock recruitment relationship, and $\mathbf{move}_{y,1} = \mathbf{0.5}$. The upper plots show the median while the lower plots show the 5, 10 and 15%ile for the west component over a narrower range on both axes. These plots correspond to the higher starting point in 2018. The grey dotted line indicates the risk threshold of the 2007 effective west component spawning biomass.

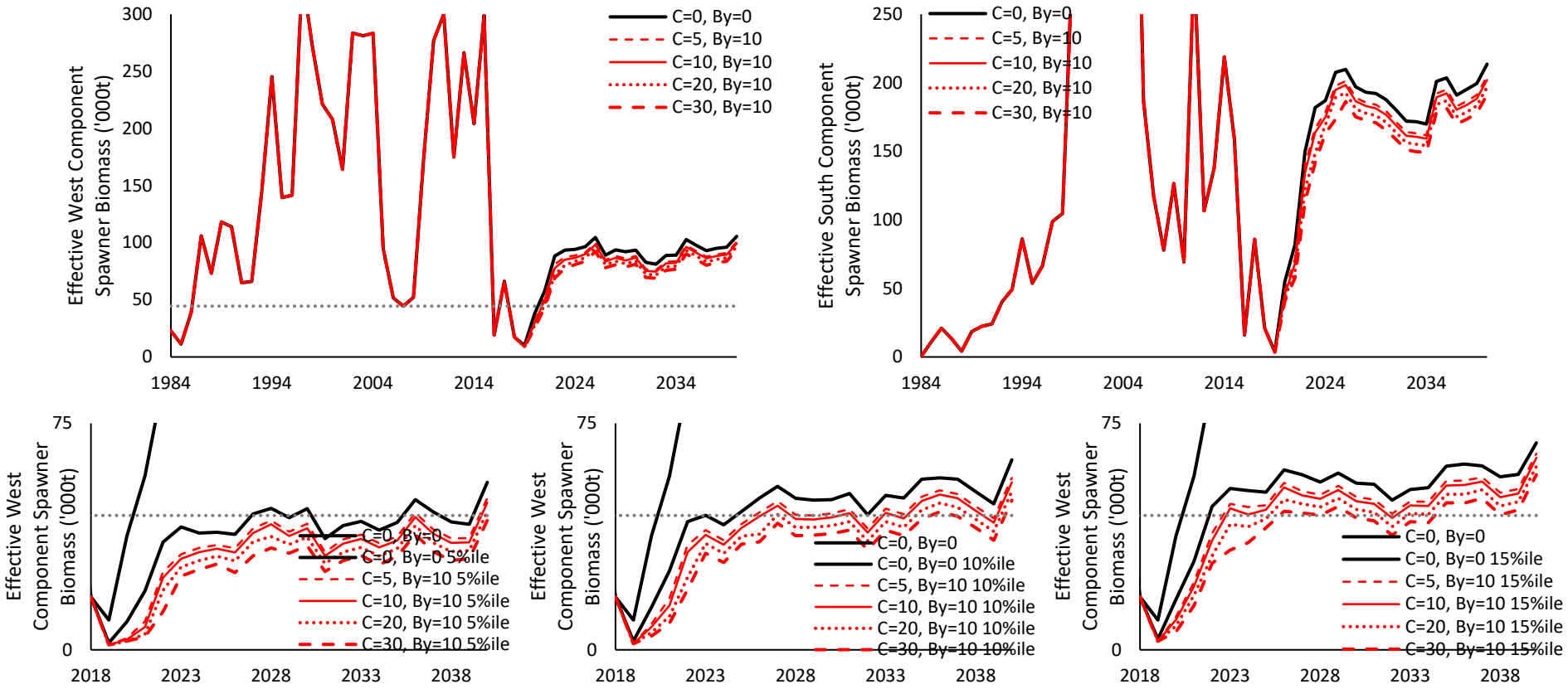

Figure B6b. As per Figure 8a, but with lower starting point in 2018.

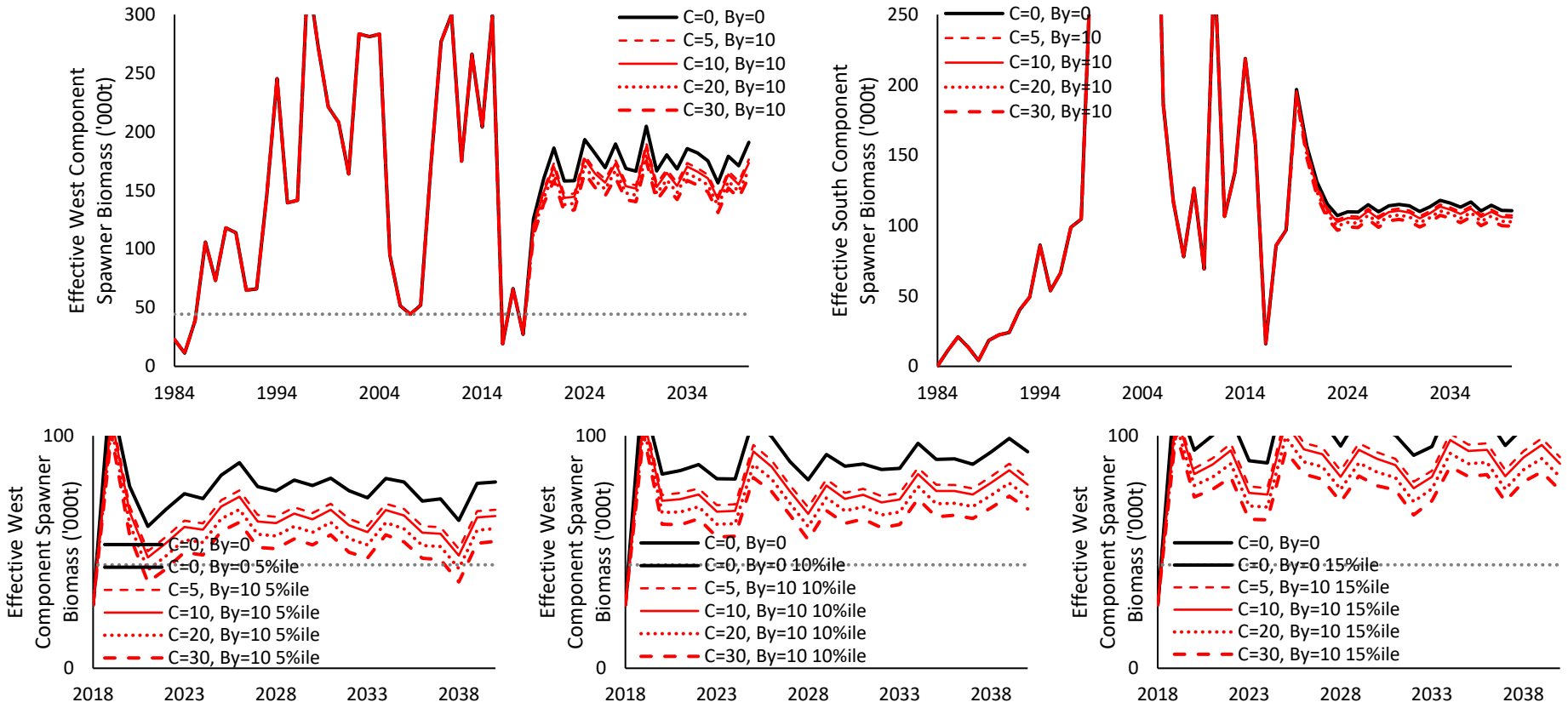

Figure B7a. Effective spawning biomass for the (left) west and (right) south components for projections assuming constant directed sardine catches of 0, 5, 10, 20 or 30 000t with recruitment drawn randomly from the past 5 years, and $\mathbf{move}_{y,1} = \mathbf{0.1}$. The upper plots show the median while the lower plots show the 5, 10 and 15%ile for the west component over a narrower range on both axes. These plots correspond to the higher starting point in 2018. The grey dotted line indicates the risk threshold of the 2007 effective west component spawning biomass.

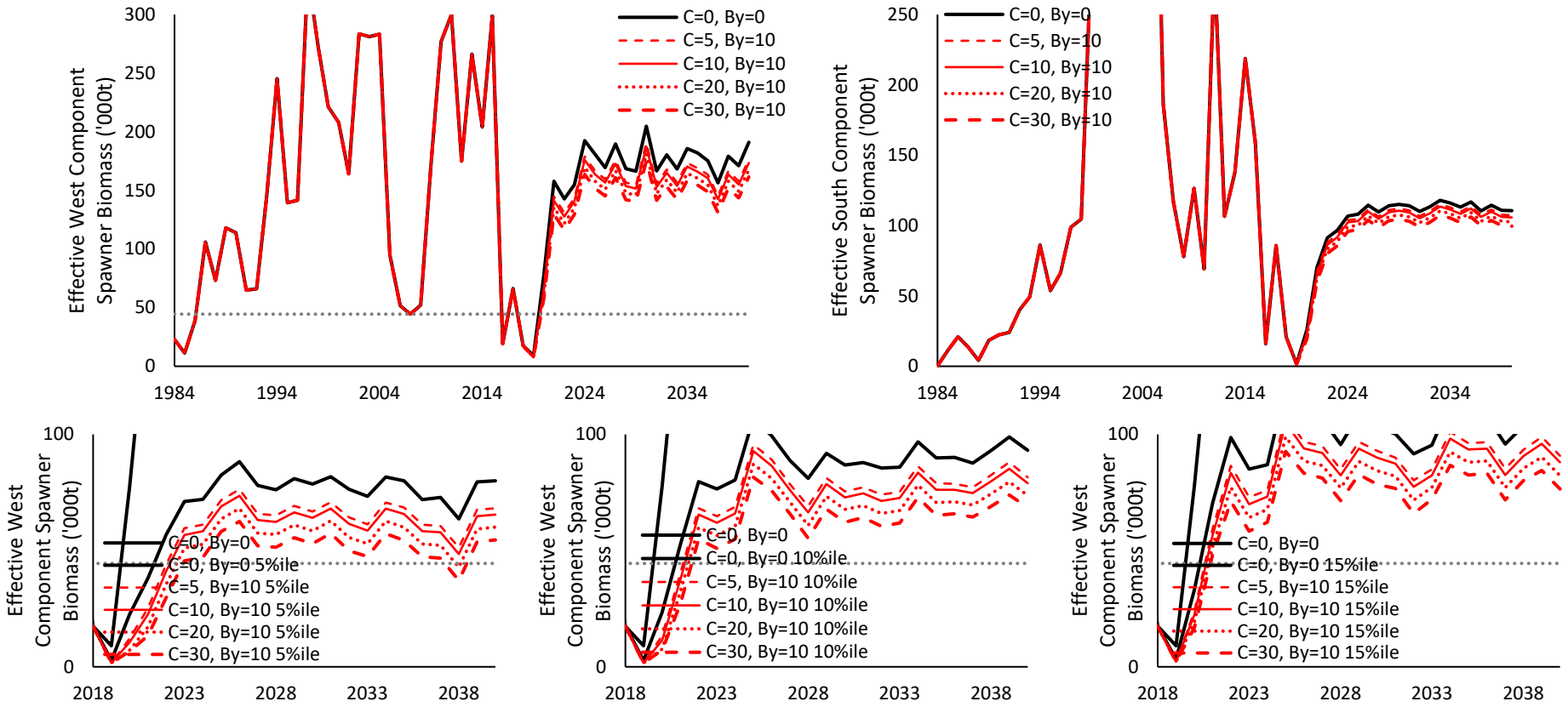

Figure B7b. As per Figure B7a, but with lower starting point in 2018.

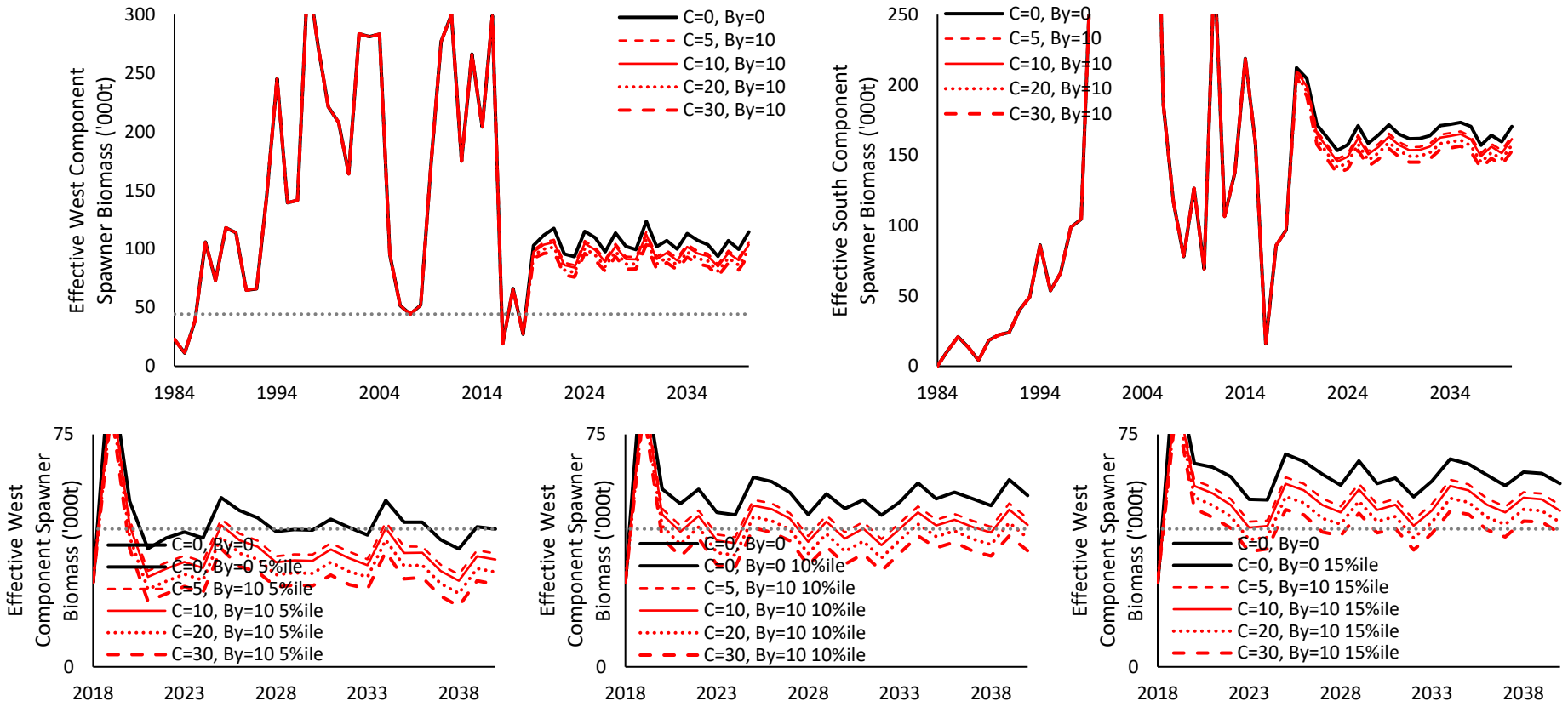

Figure B8a. Effective spawning biomass for the (left) west and (right) south components for projections assuming constant directed sardine catches of 0, 5, 10, 20 or 30 000t with recruitment drawn randomly from the past 5 years, and $\mathbf{move}_{y,1} = \mathbf{0.3}$. The upper plots show the median while the lower plots show the 5, 10 and 15%ile for the west component over a narrower range on both axes. These plots correspond to the higher starting point in 2018. The grey dotted line indicates the risk threshold of the 2007 effective west component spawning biomass.

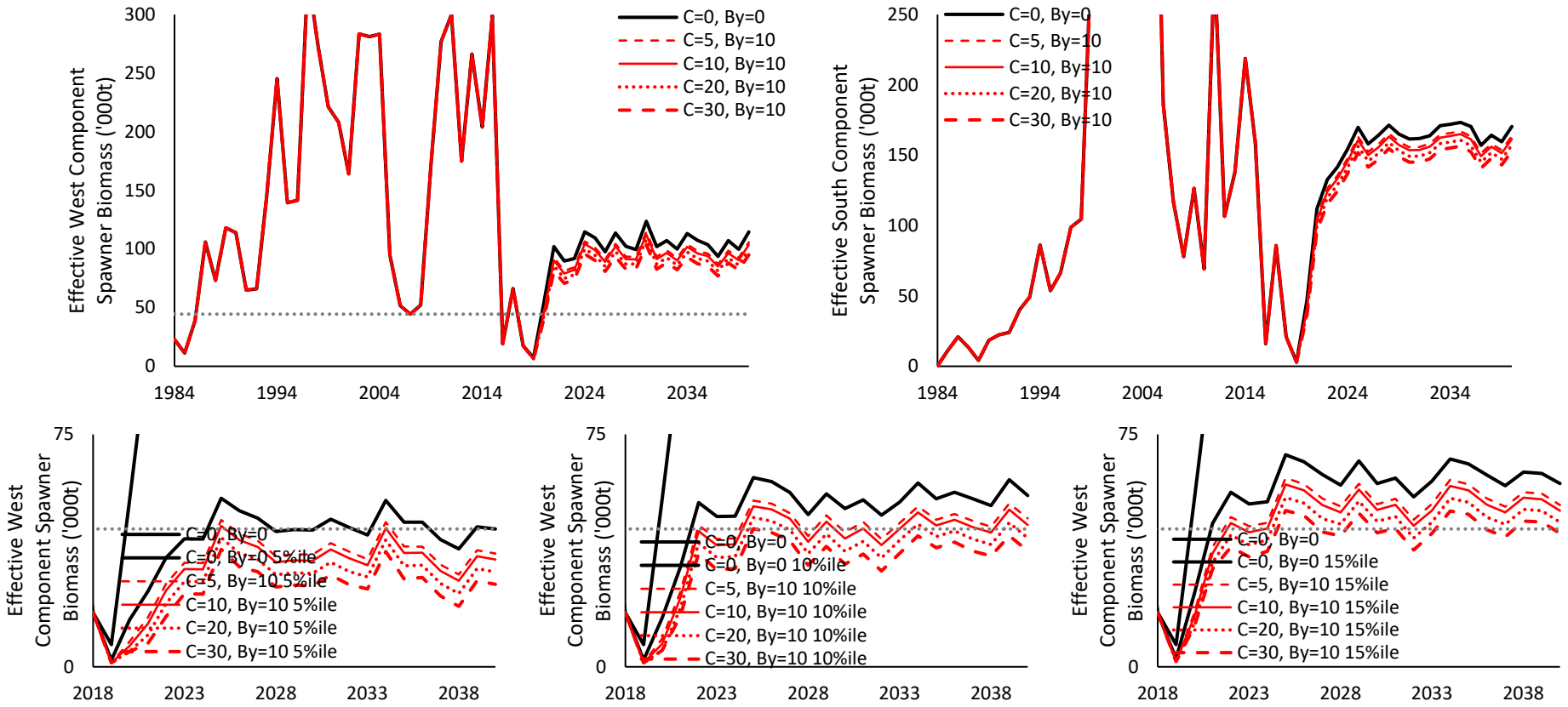

Figure B8b. As per Figure B8a, but with lower starting point in 2018.

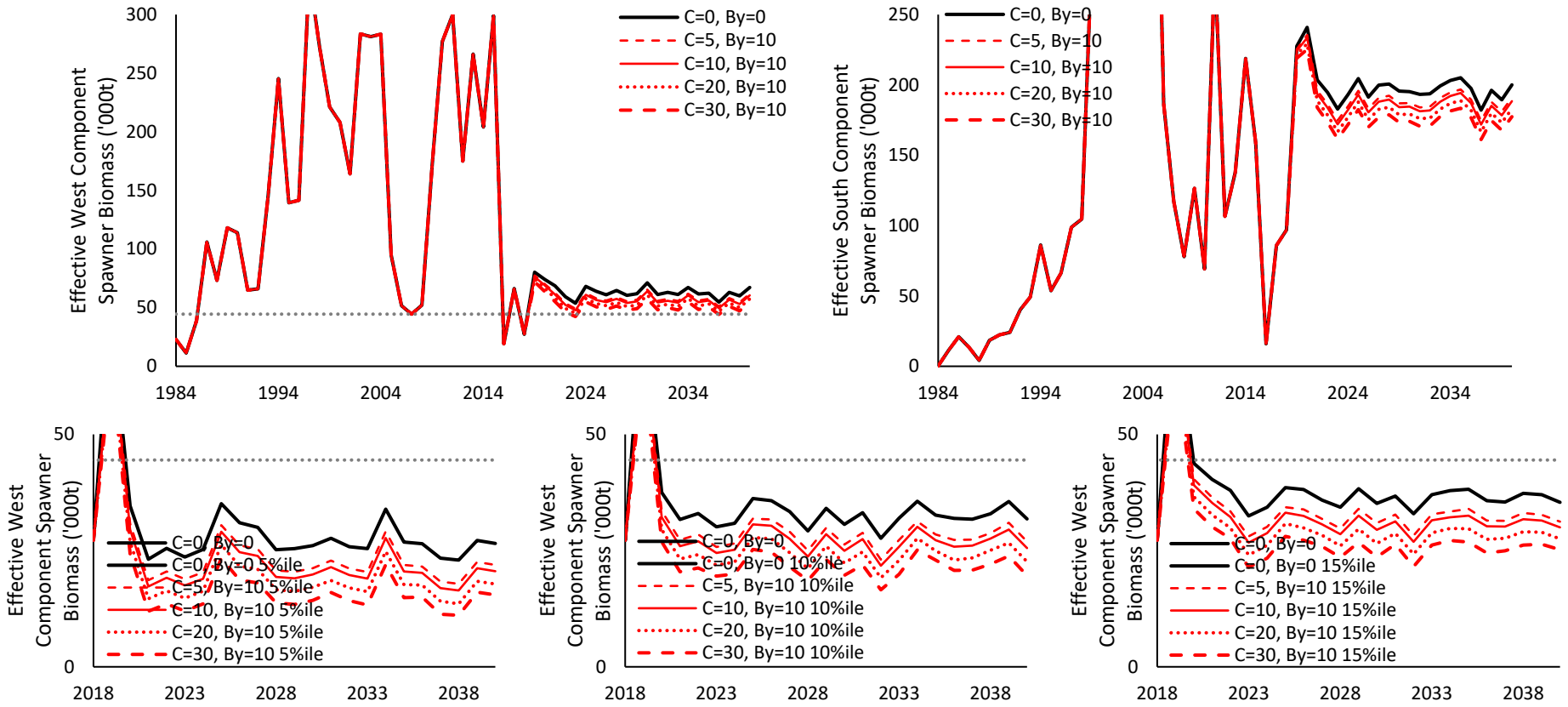

Figure B9a. Effective spawning biomass for the (left) west and (right) south components for projections assuming constant directed sardine catches of 0, 5, 10, 20 or 30 000t with recruitment drawn randomly from the past 5 years, and $\mathbf{move}_{y,1} = \mathbf{0.5}$. The upper plots show the median while the lower plots show the 5, 10 and 15%ile for the west component over a narrower range on both axes. These plots correspond to the higher starting point in 2018. The grey dotted line indicates the risk threshold of the 2007 effective west component spawning biomass.

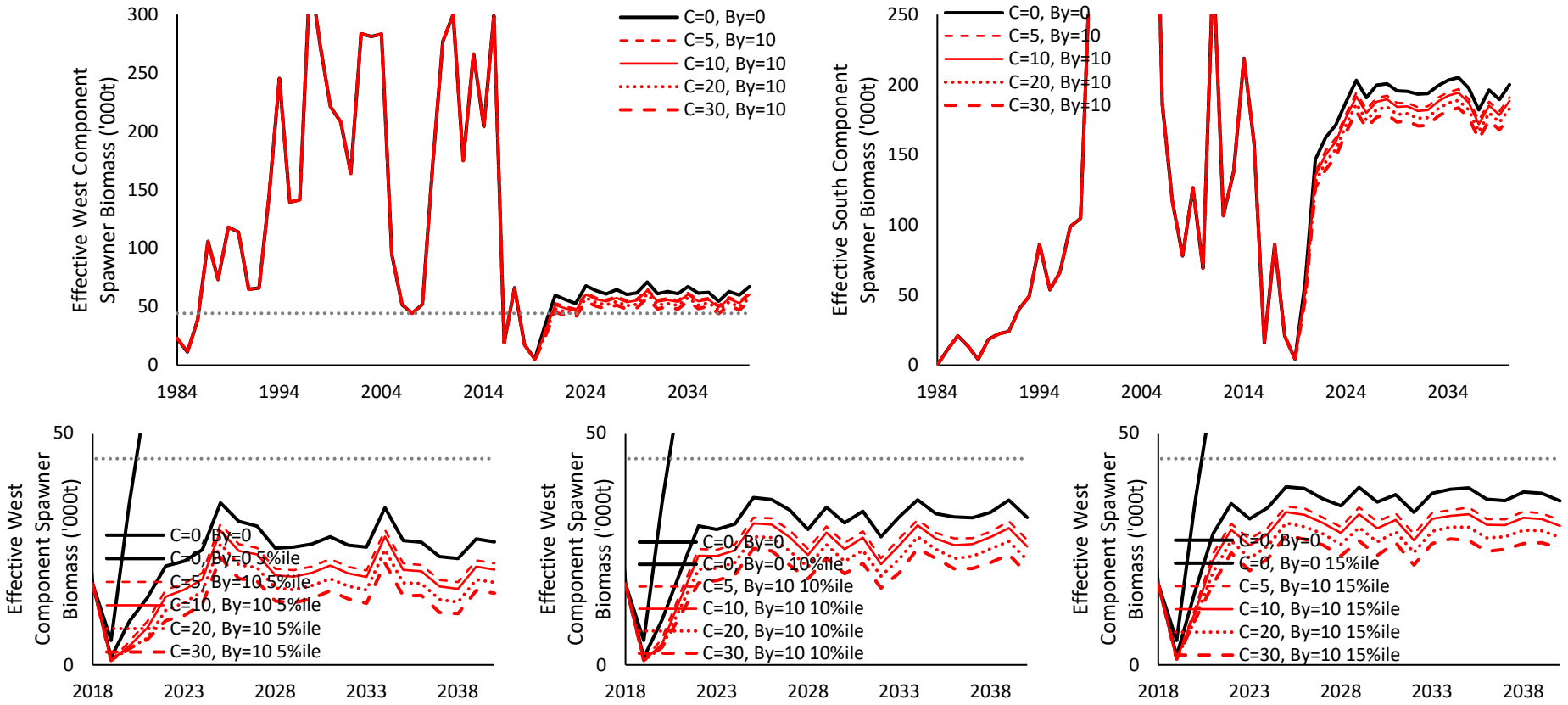

Figure B9b. As per Figure B9a, but with lower starting point in 2018.